Flinders UNIVERSITY
ADELAIDE · SOUTH AUSTRALIA

Pulse wave amplitude drops as a sensitive marker of cardiovascular system activation during sleep

By

Félix Decup

Thesis
Submitted to Flinders University
for the degree of

Master of Engineering by research

College of Science and Engineering

December 2020

CONTENTS

LIST OF FIGURES

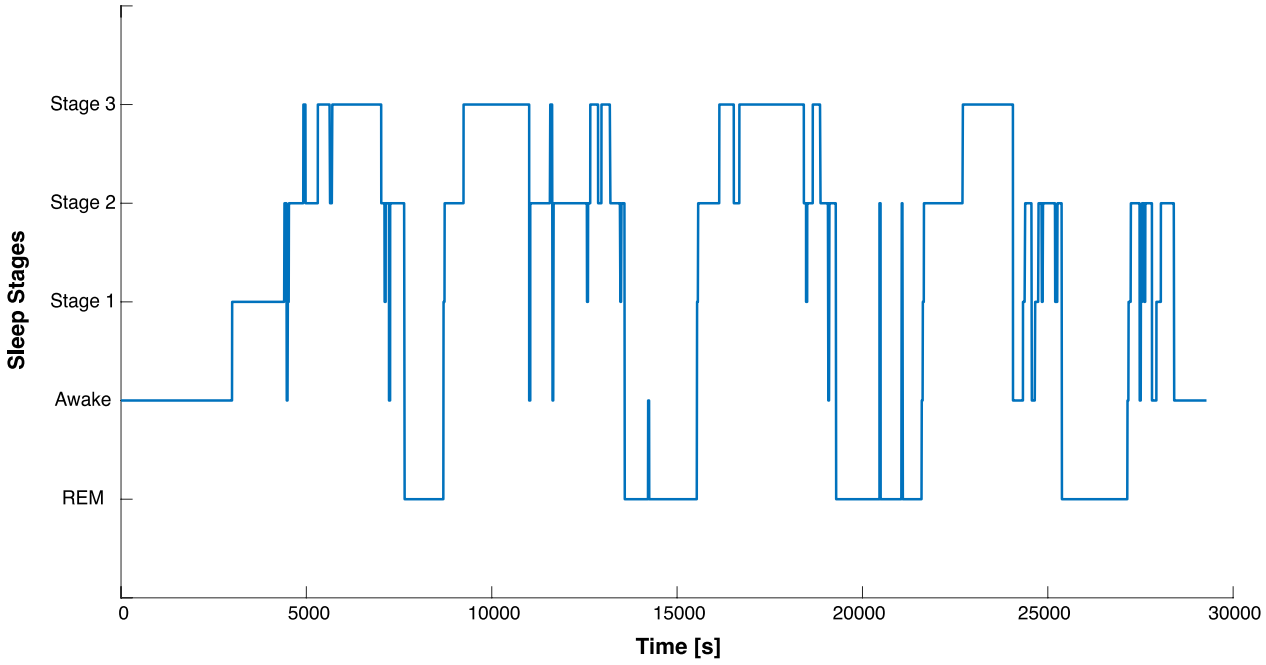

LIST OF TABLES

SUMMARY

Background: Chronically disturbed or reduced sleep is associated with adverse health outcomes. Pulse wave amplitude (PWA)-drops during sleep indicate that vasoconstriction responses detectable using pulse oximetry could be associated with cardiovascular disease and be useful clinical markers of sleep disruption.

Objectives: To develop an automated PWA-drop detection algorithm for exploration of 1) the relationship between PWA-drops and clinical cardiovascular outcomes in general population samples and 2) the disruption of sleep due to environmental noise.

Methods: An automated algorithm to detect PWA-drops from pulse-oximeter photoplethysmogram responses was developed, incorporating inter-pulse baseline de-trending and moving average-based criteria for detecting the onset, offset, duration and area under curve (AUC) of each PWA-drop, and the number of drops per hour of sleep. Effects of noise on traditionally scored electroencephalogram (EEG) sleep arousals >3-sec and PWA-drops were studied during two nights of sleep experiments in 25 participants (11 males, aged 26.5±16.4 years, range: 18-75 years and 14 females, aged 24.1±9 years, range: 19-55 years) exposed to 20-sec environmental noise stimuli (windfarm and traffic noises) at levels ranging from 33 to 48 dB(A). Associations between sound pressure level and PWA-drops, controlled for noise type and conventionally scored sleep stage, were investigated using survival analysis. To explore the relationship between PWA-drops and cardiovascular pathophysiology, two large-population based cohorts were also studied: the HypnoLaus cohort of 2162 individuals who underwent home-based sleep studies from a general population in Lausanne, Switzerland; and the Men Androgen Inflammation Lifestyle Environment and Stress (MAILES) cohort which included home-based polysomnography from 752 men in Adelaide, Australia. A possible association between PWA-drop features (number of PWA-drops per hour, mean duration and mean AUC), and prevalent hypertension and/or cardiovascular disease in these cohorts was explored using multivariate-adjusted logistic regression analysis.

Results: PWA-drops were more sensitive predictors of the presence versus absence of noise stimuli than traditionally scored EEG arousals at lower sound pressure level during stage 2, 3 and REM sleep (Control vs 48 dBA: HR_{PWA} = 2.9 [2.2 – 3.8] and HR_{EEG} = 2.5 [1.5 – 4.2], Control vs 39 dBA: HR_{PWA} = 1.5 [1.1 – 2.0] and HR_{EEG} = 1.1 [0.6 – 2.1], Control vs 33 dBA: HR_{PWA} = 1.1 [0.8 – 1.5] and HR_{EEG} = 0.6 [0.3 – 1.3], respectively). The mean AUC of PWA-drops was the only feature consistently associated with the hypertension prevalence in both the HypnoLaus and MAILES cohorts (OR [95%CI] = 1.42 [1.03-1.96] and OR = 1.84 [1.10-3.08], respectively, pooled cohorts OR = 1.58 [1.21-2.07]). However, no consistent association was observed from pooled datasets between the prevalence of cardiovascular disease and PWA-drop features (number of PWA-drops per hour: OR = 0.73 [0.46-1.17], mean duration: OR = 0.82 [0.53-1.28], and mean AUC: OR = 0.90 [0.55-1.47]).

Conclusions: Automatically scored PWA-drops during sleep are a sensitive marker of cardiovascular system activation responses to noise and in two large population cohorts are associated with hypertension. Further studies are clearly warranted to better understand the nature of potential causal relationships between prolonged environmental noise exposure, cardiovascular disturbances in sleep more generally, and potential long-term adverse health effects such as hypertension.

DECLARATION

I certify that this thesis does not incorporate without acknowledgment any material previously submitted for a degree or diploma in any university; and that to the best of my knowledge and belief it does not contain any material previously published or written by another person except where due reference is made in the text.

Signed.....

Date.....15/12/2020.....

ACKNOWLEDGEMENTS

The work presented in this thesis could not have been completed without the unwavering support of my supervisors Dr Kristy Hansen, Dr Branko Zajamsek and Professor Peter Catcheside. Thank you for all you have taught me, for sharing your experience and knowledge, for your support and encouragement, and this great opportunity that you gave me.

Many people assisted in the conduction of the studies presented here. My thanks are extended to: Dr Gorica Micic, Claire Dunbar, Tessa Liebich, Duc Phuc Nguyen, Mahmoud Ahmed Alamir and Bastien Lechat for accommodating the recruitment and data collection process, and the Adelaide Institute for Sleep Health team for their guidance, support and the incredible atmosphere in this laboratory.

Finally, thank you to my friends and family for their constant love, support and encouragement.

CHAPTER 1 - OVERVIEW

1.1 Introduction

When asleep, the human body is in a vulnerable state and thus autonomic nervous system regulated "fight-or-flight" responses are potentially vitally important for surviving local and environmental threats that may arise during sleep. A major component of this response is a transient blood pressure surge necessary to support increased cardiovascular and metabolic system activity. Blood pressure surges are achieved partly via changes in heart rate and stroke volume, but predominantly via vasoconstriction in peripheral skin vascular beds that shunts blood away from the periphery towards the heart, lungs, active muscles and brain (Schnall et al., 1999).

Subtle markers of sleep microstructure associated with these cardiovascular responses are potentially more sensitive markers of sleep disturbance than traditional direct electroencephalographic markers of sleep stage changes or cortical micro-arousals (Grote and Zou, 2017). Whilst these episodes of autonomic disturbance might be critical for survival, over-activation of the cardiovascular system might increase risk factors for hypertension and cardiovascular disease. Therefore, one of the main purposes of this project was to assess if finger vasoconstriction could be a marker of cardiovascular system activation which increases the risk of developing hypertension and cardiovascular disease. Moreover, finger vasoconstriction could also be a sensitive marker of noise disturbance during sleep and thus potentially a useful marker of sleep disturbance to acoustic stimuli, which were also investigated in this project.

1.2 Overview of the sleep process

Clear distinction exists between physiological states whilst awake and asleep and thus this review starts with an overview of the sleep as conventionally scored using current American Association of Sleep Medicine (AASM) criteria (Berry et al., 2012).

1.2.1 Measuring sleep: Polysomnography

Polysomnography (PSG) is considered the gold standard measurement of sleep and simultaneously records multiple physiological parameters such as brain electrical activity with at least one electroencephalogram (EEG) channel, left and right electro-occulograms (EOGs), an electromyogram (EMG) usually from the chin, an electrocardiogram (ECG), and usually arrange of respiratory-related signals including oximetry to assess breathing during sleep. Although often not recorded, a useful signal also available through oximetry is a finger photoplethysmogram (PPG) (Figure 1), which represents the pulsatile component of light transmittance through the finger vascular bed underneath the oximeter probe.

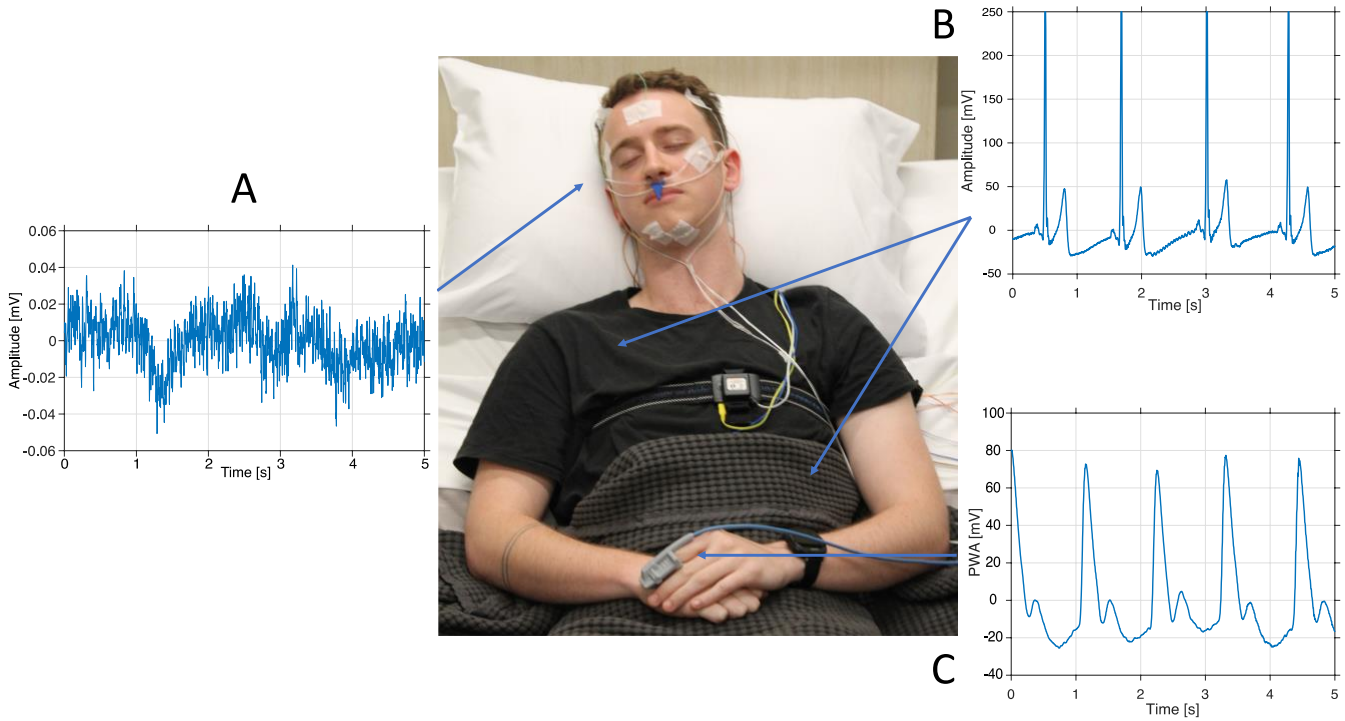

Figure 1: Polysomnography set-up. A) a 5 s example of an electroencephalogram signal from one lead on top of the head (called F3 in the 10-20 system of polysomnography), B) a 5 s example of an electrocardiogram signal from two leads positioned on the chest, one on the top left and one on the bottom right (ECG lead II), and C) a 5 s example of a photoplethysmogram signal recorded from a finger pulse oximeter.

1.2.2 Sleep Structure

Sleep structure is manually scored according to standardised scoring rules originating from the 1960s (Kales and Rechtschaffen, 1968). Sleep is typically scored in 30-second long epochs classifying sleep macro-structure into non-rapid eye movement (NREM) sleep divided into 3 stages N1, N2 and N3, and rapid eye movement (REM) sleep (Figure 2):

- N1 corresponds to light sleep during which brain activity begins to slow down (theta activity, frequency band between 3 and 8 Hz) from wake (low amplitude with faster alpha waves, frequency band between 8 and 12 Hz). N1 usually occupies around 5% of the total sleep time.
- N2 is characterised by the appearance of K-complexes (transient EEG slow wave activity) and short bursts of EEG spindles (bursts of 12-14 Hz activity) and typically makes up approximately 50% of sleep.
- N3 is commonly referred to as “deep sleep” or slow wave sleep (SWS) and occupies around 20 - 25% of the total sleep time. N3 is characterised by large amplitude slow wave activity (0.5-2 Hz) and is considered to be the most restful stage of sleep (Muzet, 2007).

- REM sleep is characterised by more active brain-wave activity than in N2 and N3 and is accompanied by characteristic rapid eye movements. REM occurs for 20 - 25% of the total sleep time and is strongly associated with daytime mental functioning and memory processing (Muzet, 2007).

Sleep is typically composed of multiple sleep cycles lasting between 40 to 90 min, repeating 4 to 6 times over a full night of sleep, as shown in Figure 2. Two distinct features can be distinguished in each sleep cycle: 1) an ascending slope, where sleep stages change from stage 1 towards stage 3, and 2) a descending slope, where sleep changes from deeper to lighter stages (sleep stages 3 toward stage 1 and REM). Periods of N3 typically become shorter cycle after cycle, whereas periods of REM usually lengthen.

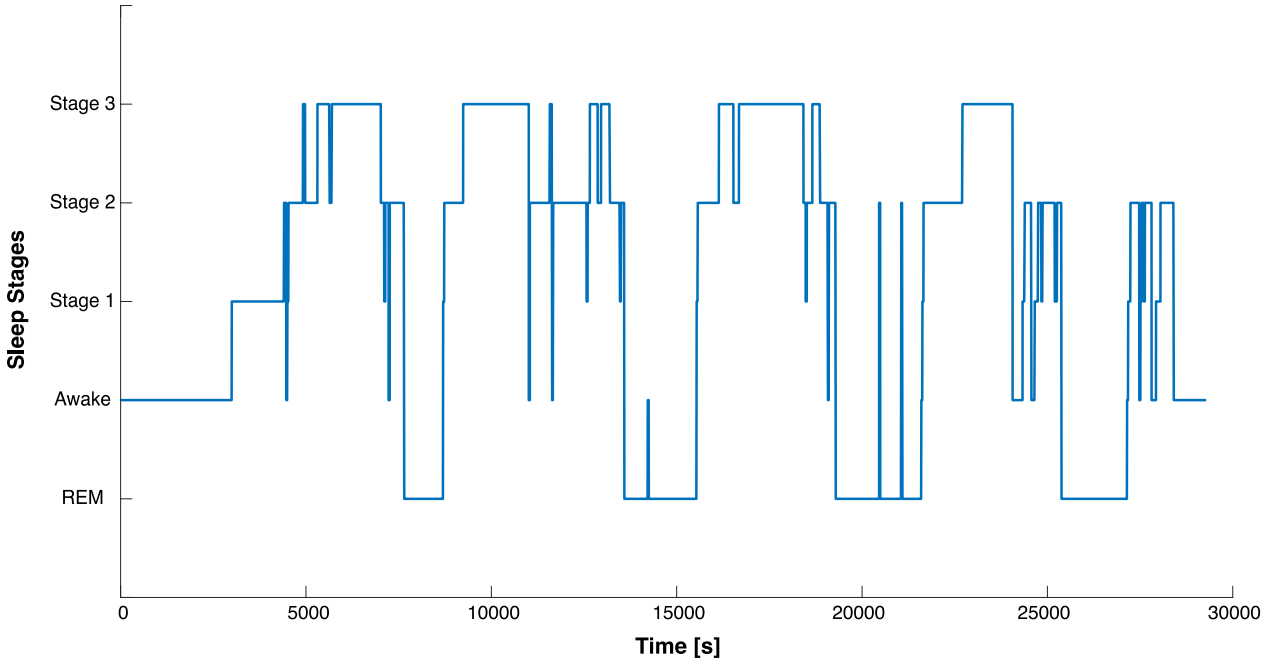

Figure 2: Example of a hypnogram.

However, conventional sleep scoring in 30-seconds epochs does not capture more subtle changes that occur during sleep and fails to predict important clinical outcomes such as adverse cardiovascular events (Rosenthal and Dolan, 2008).

1.2.3 Cardiovascular system during sleep

The autonomic nervous system (ANS) has two main branches which both control the cardiovascular system, typically with antagonistic effects, through the parasympathetic nervous system and the sympathetic nervous system (SNS). The ANS maintains body homeostasis and allows the body to respond to changes in the environment. The parasympathetic nervous system predominantly operates to conserve and store energy, whilst the SNS dominate “fight-or-flight”

responses (McCorry, 2007). These systems operate largely unconsciously to regulate the physiology of the body, including heart hate (HR) and skin vasomotor responses underpinning finger pulse wave amplitude (PWA). HR is controlled by both the parasympathetic nervous system and the sympathetic nervous system whilst PWA is mainly controlled by the sympathetic nervous system (Grote and Zou, 2017, Di Nisi et al., 1990).

As sleep deepens towards slow wave sleep, an increase in heart rate period can be observed (Silvani, 2008), which is attributed to an increase in parasympathetic activity (Grote and Zou, 2017, Baust and Bohnert, 1969), coupled with a decrease in arterial blood pressure of about 10% (Silvani et al., 2016, Silvani and Dampney, 2013). In REM sleep, ANS activity varies greatly with phasic changes in sympathetic and parasympathetic discharge (Zoccoli and Amici, 2020). While the neuronal/physiological mechanism of these changes are unclear (Silvani et al., 2016), they are clearly observable with non-invasive markers derived from ECG and photoplethysmography sensors. Cardiovascular changes are prominent enough for some groups to have investigated markers of sleep depth and quality based only on ECG leads (Thomas et al., 2018, Lee et al., 2014, Brandenberger et al., 2001, Thomas et al., 2005).

Interestingly, when normal NREM expression is prevented, the sympathetic activity remains as high as wakefulness (Zoccoli and Amici, 2020). This results in over-activity of the sympathetic nervous system during NREM sleep and could potentially represent a risk factor for cardiovascular disease.

1.2.4 Pulse wave signal

Photoplethysmography is a non-invasive and inexpensive simple optical technique used to detect volumetric changes in peripheral blood circulation, usually at the finger. The PWA-drop derived from photoplethysmography, occurs due to a decrease of blood flow in the finger which is mostly due to increased skin sympathetic activation and vasoconstriction (Grote and Zou, 2017), and corresponds to a marked decrease in the PWA signal, lasting around 30 - 40 seconds, as shown in Figure 3.

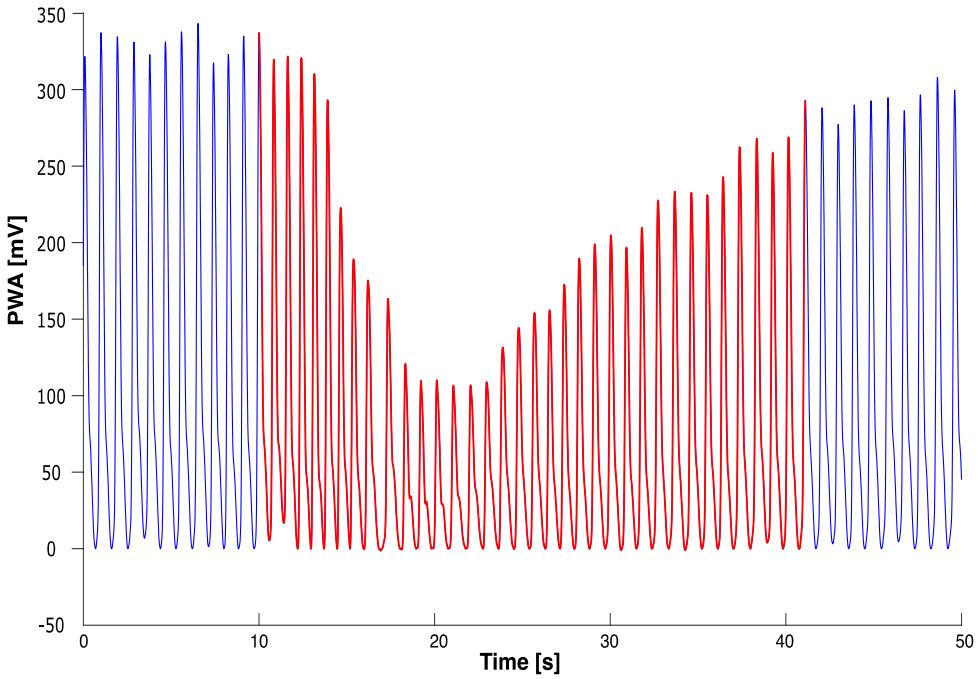

Figure 3: Example of a PWA-drop.

While there is a great potential for PWA-drops to contain valuable information about the cardiovascular system during sleep (Terrill, 2020), this signal has received very little attention compared to ECG signals. The potential of PWA-drops as a marker of sleep disturbance has been mostly studied in response to acoustic stimuli (Griefahn, 2017, Catcheside et al., 2002, Schnall et al., 1999) or apnoeic events (Grote et al., 2003). A small number of studies have investigated associations between pulse wave amplitude markers and clinical outcomes (Hirotsu et al., 2020, Grote et al., 2011). Thus, while PWA markers have the potential to provide a useful marker of cardiovascular health, stronger evidence is required to support potential clinical utility.

CHAPTER 2 - LITERATURE REVIEW

2.1 Pulse wave amplitude drop detection

Few algorithms have been developed to automatically detect PWA-drops (Betta et al., 2020, Grote et al., 2011, Pillar et al., 2002). Pillar et al. (2002) developed their algorithm on a scored dataset of 40 patients where a PWA-drop was scored when the amplitude signal decreased by at least 50% relative to the baseline. Betta et al. (2020) used a dataset of 16 participants with two human scorers. The threshold for scoring a PWA-drop was defined as an instant when the pulse wave amplitude signal decreased by at least 30% relative to the baseline. Grote et al. (2011) developed a matching pursuit algorithm for cardiovascular risk assessment with multiple variables, one of which was a decrease of 30% or more in pulse wave amplitude signal compared with the baseline. However, no detection validation was done on this variable alone. Largely arbitrary cut-offs with no established “gold standard” methodology or clinical outcomes potentially related to vasoconstrictor responses makes it difficult to decide what approach may be clinically more useful. Betta et al. (2020) are the only group to have validated an algorithm solely based on automated PWA-drop detection.

2.2 Mortality and cardiovascular risk associated with disturbed sleep

Sleep is a fundamentally important biological process underpinning good health. Evidence suggests that sleep is involved in systemic metabolic regulation and tissue growth and repair, for example, glucose regulation (Spiegel et al., 1999) or cortisol secretion (Vgontzas et al., 2004). Collectively, these experimental studies suggest that chronically disturbed or reduced sleep could impact on morbidity and mortality (Hillman et al., 2006).

Epidemiological studies suggest that a reduced total sleep time, reduced slow wave sleep, and a high number of awakenings are associated with a greater risk of hypertension, cardiovascular events and all-cause mortality (Zinchuk et al., 2018, Javaheri et al., 2018, Kendzerska et al., 2014). Furthermore, multiple sleep disorders, such as sleep disordered breathing (Shahar et al., 2001, Grote et al., 1999, Nieto et al., 2000), insomnia (Bertisch et al., 2018, Chen et al., 2013) and restless leg syndrome (Li et al., 2018), have all been associated with a greater risk of adverse health outcomes such as hypertension or cardiovascular disease.

Only one up-to date study showed an association between PWA-drop characteristics and hypertension and cardiovascular events (Hirotsu et al., 2020). The number of PWA-drops per hour (index), the mean duration of PWA-drops and the mean area under the curve were shown to be associated with cardiometabolic outcomes. Furthermore, the mean normalised (with total sleep time) number of PWA-drop per hour lowest quartile had significantly higher odds ratio for

hypertension, cardiovascular events and diabetes compared to those in the highest quartile. Similar results have been observed by Sommermeyer et al. (2014), where a lower number of PWA-drops per hour was associated with an increased cardiovascular risk.

2.3 Impact of environmental noise on sleep

Environmental noise has been associated with cardiovascular damage and sleep disturbance as depicted in Figure 4 and is a growing concern for public health (World Health, 2018, Ahn et al., 2015).

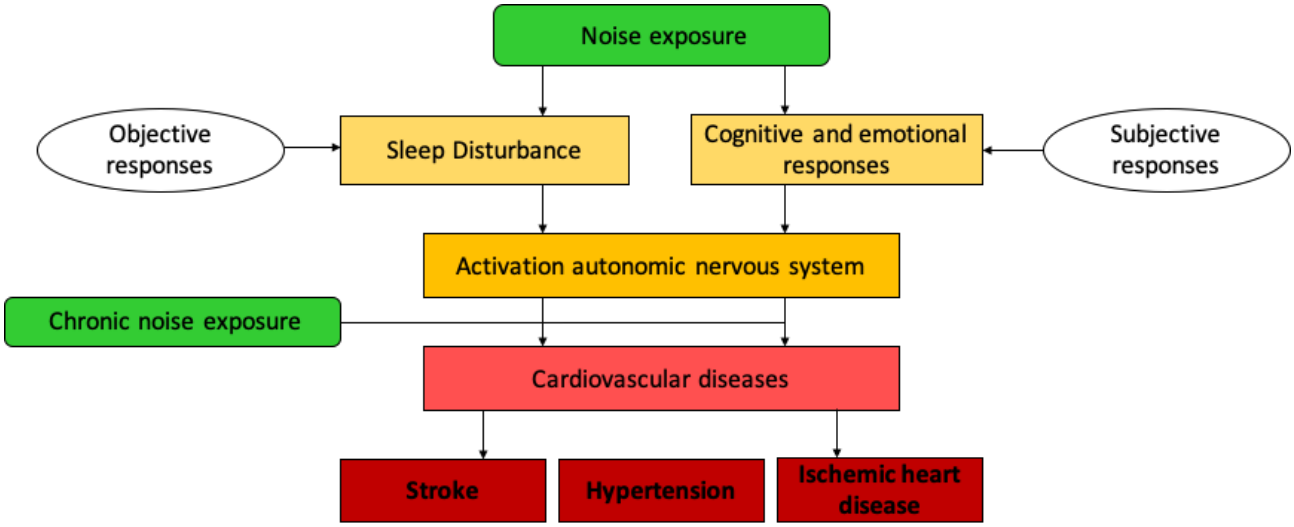

Figure 4: Human health issues due to environmental noise.

2.3.1 Cardiovascular risk associated with environmental noise exposure during sleep

Environmental noise is commonly quantified by its sound pressure level measured in dB(A). Guidelines recommend not exceeding 45 dB(A) more than 10 to 15 times a night and/or a threshold above 30 dB(A) for long periods during the night (Ahn et al., 2015). Road traffic noise (RTN) is the most common environmental noise as more than 30% of the EU population is exposed to RTN exceeding 55 dB(A) during night time (Berglund et al., 1999). New guidelines from the WHO recommend reducing RTN below 45 dB(A) L_{night} as higher levels have been associated with adverse effects on sleep (World Health, 2018). Recently wind farm noise has been reported to be associated with sleep disturbance at sound pressure levels above 40-45 dB(A) (Basner and McGuire, 2018).

The two main acoustic characteristics of wind turbine noise (WTN) that could potentially be the most problematic for sleep disturbance are low-frequency content and amplitude modulation. Little is known about the physiological impacts of these two WTN characteristics during sleep.

Smith et al. (2020) appear to be the only research group to have studied the effect of WTN amplitude modulation on sleep and suggested that this noise component could be one characteristic of the noise particularly disturbing to sleep.

Several studies speculate that chronic exposure to noise could affect metabolic and cardiovascular system health (Munzel et al., 2018, Basner et al., 2014, Babisch, 2011, Berglund et al., 1999). Potentially permanent metabolic changes could promote a higher risk of cardiovascular disease, myocardial infarction or stroke (Basner et al., 2014, Babisch, 2011) and/or chronic disorders such as increased risk of hypertension, ischemic heart diseases and atherosclerosis (Munzel et al., 2018, Basner et al., 2014, Babisch, 2011, Berglund et al., 1999). Basner et al. (2014) observed that autonomic arousal, potentially one of the main risk factors for cardiovascular disease, could be caused by noise at 33 dB(A) and would probably depend on the frequency of occurrence of events. Héritier et al. (2017) also noted that the intermittency of traffic events above the background level could be an important trigger for cardiovascular disease.

To date, noise-related sleep disturbance has been mainly assessed by subjective measures (Pirrera et al., 2010), where people are requested to recall and answer questions regarding their previous night's sleep. Questionnaire measurement depends on how well the person remembers the night and are subject to potential participant and recall bias (Öhrström and Skånberg, 2004). Thus, it is difficult to conclude with subjective measurements if self-reported sleep disturbance reflects that individuals are more sensitive to noise, or if they associate wake with hearing unwanted noise (Muzet, 2007). Therefore, objective measurements such as EEG to objectively determine sleep stages and awakenings, and potentially electrocardiogram and finger pulse oximetry related responses may be more useful and reliable markers of sleep disturbance due to noise.

2.3.2 Objective responses to environmental noise

Autonomic or cortical responses to noise during sleep such as heart rate (HR), vasoconstriction, event-related EEG arousals and awakenings seem to depend on acoustical characteristics, however their relative prominence is not well known (Smith, 2017, Basner et al., 2014). It might be an advantage to use the number and acoustic properties of single noise events to better predict nocturnal sleep disturbance (Basner et al., 2010). Moreover, the difference in sound pressure levels between noise stimuli and background noise, as well as the time interval between two noise events influence physiological responses (Berglund et al., 1999). Arousals, awakenings and body movements, among other parameters are physiological events that occur during normal nights and only become a problem when frequent (Basner et al., 2014). However, high variability among individual physiological reactions are problematic for establishing fixed

limit values to be defined for the activation of the autonomic nervous system when exposed to traffic noise (Basner et al., 2010).

2.4 Markers of noise-induced sleep disturbances

2.4.1 Physiological macro-structure responses

Vallet et al. (1983) observed a reduction in deep sleep duration in response to noise exposure due to an increased number of awakenings and sleep state changes. These authors observed that the average traffic noise level that provoked an awakening was 50.3 dB(A) while for a sleep state change 48.5 dB(A) was sufficient. The higher the noise level, the more the sleep was likely to be disturbed (Vallet et al., 1983).

Griefahn et al. (2006) found that traffic noise at levels equal to or above 39 dB(A) affected slow wave sleep (SWS) latency, wake after sleep onset (WASO), sleep efficiency, and the percentage of time spent in wakefulness and stage 1. Eberhardt et al. (1987) found SWS was reduced to 22% (5 min) from the baseline quiet condition and delta wave activity decreased by 10%, indicating slow wave activity and a corresponding higher susceptibility to noise disturbance during sleep. Additionally, 108 changes to lighter sleep were recorded and only 18 were associated with traffic noise. Furthermore, Basner et al. (2018) reported that sleep disturbance due to noise includes reduced sleep continuity, delayed sleep onset, awakenings, reduced N3 and REM sleep. Changes in the macrostructure of sleep are subtle and EEG likely contains more information such as micro-arousals and K-complexes that may help to better inform sleep disturbance effects.

2.4.2 Cardiovascular system responses

Cardiovascular surges in response to noise stimuli are another area of study in noise-induced sleep disturbance that have been associated with an increased risk of cardiovascular disease (Basner et al., 2014). Autonomic nervous system activation responses to noise stimuli do not appear to habituate, even after a long exposure time (Muzet, 2011).

Cardiovascular responses depend on the sleep stage in which noise events occur. Griefahn et al. (2017) found that cardiac noise-induced responses (HR and vasoconstriction) were more pronounced in Stage 2 and REM sleep compared to deep or SWS. However, waking from deep sleep induced a stronger response than waking up from lighter stages such as REM or Stage 1. Johnson et al. (1967) found that HR responses due to noise, with a tone of 1000 Hz at 30-35 dB above the hearing threshold, were less sensitive in SWS compared to Stage 2 and REM sleep. Bach et al. (1991) presented three different noises during the night, one of a car at 64 dB(A), one of a motorcycle at 67 dB(A) and one of a truck at 71 dB(A). The results showed that the HR

noise-induced responses were larger and more frequent in Stage 2 and in REM sleep compared to SWS. Whilst finger PWA noise-induced responses were only larger and more frequent in Stage 2 compared to SWS. On the other hand, Tassi et al. (2010) reported that HR responses were not dependent on sleep stages and the PWA response rate decreased during REM sleep compared to Stage 2 and SWS. Nevertheless, as suggested by Johnson et al. (1967), during REM sleep the PWA evoked response rates could be smaller due to more frequent spontaneous PWA responses which could then "block" the evoked responses. Tassi et al. (2010) also found that PWA responses were larger in SWS than Stage 2 and REM sleep for noise at 50 dB(A) L_{Aeq} with peaks at 66 dB(A). This is possibly because individuals were awakened multiple times and the average response could then have been larger in SWS (Griefahn, 2017). Nonetheless, a significant drop in PWA was observed in Stage 2, SWS and REM sleep by multiple research groups (Johnson and Lubin, 1967, Bach et al., 1991, Tassi et al., 2010). Furthermore, Griefahn et al. (2017) observed that autonomic arousal started before noise onset, for example the HR was particularly disturbed by noise during sleep, at least in the case of full awakenings, if noise occurred during a spontaneous arousal, suggesting that noise onset during brief arousals may promote progression to full awakenings.

Keefe et al. (1971) reported that PWA responses showed a 10 dB(A) lower threshold than the HR response. Di Nisi et al. (1990) showed that the HR and PWA responses were proportional to the noise intensity regardless of the noise types. For instance, airplane (67.7 dB(A)) and railway (68.2 dB(A)) noise had larger responses compared to truck (61.9 dB(A)) and motorcycle noise associated with pass-by events (52.7 dB(A)). Similarly, Tassi et al. (2010) found that the PWA response and the PWA latency (from the start of the response to the minimum amplitude of the drop) both gradually increased as a function of noise intensity. However, the PWA minimum varies between experiments, with values between 37 and 40% drop from baseline for train noise exposure ranging from 51 to 66 dB(A) (Tassi et al., 2010), and between 45 and 65 % drop for exposure to different types of transportation noise, ranging from 52 to 69 dB(A) (Di Nisi et al., 1990).

2.5 Pulse wave amplitude drop – a more subtle marker of noise disturbance

HR and PWA responses are mediated by different parts of the autonomic nervous system. The HR response is influenced by the parasympathetic and sympathetic nerves innervating the heart itself whilst PWA responses appear to be innervated mostly by sympathetic nerves supplying skin vascular beds.

However, during sleep, the HR and PWA responses seem to be closely related: when HR accelerates, PWA also tends to fall (Di Nisi et al., 1990). It has been hypothesised that the HR response could be an indicator of a stress response to noise, whereas the PWA response may

be more closely related to both cardiovascular and auditory protective mechanisms such as the auditory reflex (Kryter and Poza, 1980). These differences could explain why the PWA response appears to be more sensitive to noise, the threshold being 10 dBA lower than the HR response in Stage 2 and SWS (Keefe et al., 1971).

Di Nisi et al. (1990) reported that they could not establish a clear relationship between the HR and PWA responses to transportation noise-exposure stimuli during wake. However, during sleep, the authors showed that the HR and PWA responses to noise were similar as shown in Figure 5. PWA decreases seem to be an indication of activation due to noise-exposure. Similarly, during sleep, HR acceleration might be associated with stimuli "rejection", in this case, noise stimuli. HR and PWA arousal rates due to noise-exposure are still different during sleep, even if their responses are more related.

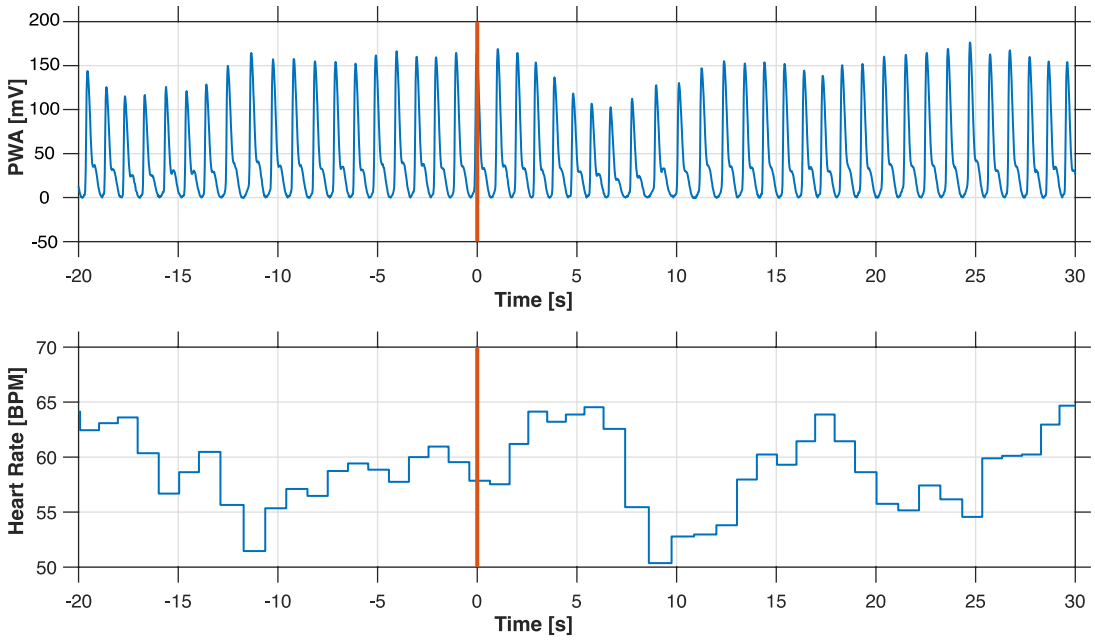

Figure 5: Cardiovascular responses due to noise during sleep. At the top is an example of PWA signal in response to noise and at the bottom is an example of the heart rate in response to noise

The HR response during sleep is either biphasic or triphasic. The HR accelerates for 3 - 5 s after noise onset (Catcheside et al., 2002) and then reaches its maximum, which may be limited by inhibition of the PNS. Then, the HR decelerates and reaches its minimum 8 - 10 s after noise onset, which could be explained by an increase in activity of the SNS (Jordan et al., 2003). Finally, HR returns to steady baseline, or in case of a triphasic response, accelerates a little more before returning to a stable baseline (Griefahn, 2017).

Skin vasoconstriction produces a drop in PWA around 3 s after noise onset, to between 20 - 50% below baseline amplitude. The minimum of the drop is reached approximately 10 s after noise

onset before finally returning back to baseline after around 30 - 40 s (Griefahn, 2017, Jordan et al., 2003, Catcheside et al., 2002). Johnson et al. (1967) scored a PWA response when it decreased by at least 20% from baseline for more than two heart beats and occurred within 2 - 6 beats after noise onset.

Bach et al. (1991) reported that the PWA showed a response to noise more frequently than the HR but had a longer latency. A PWA response is also more visible due to its decay of approximately 30 s, which is much longer than the HR response which accelerates only for a few beats over approximately 5s (Catcheside et al., 2002). Relative changes in finger PWA response were significantly greater than other cardiovascular parameters such as the finger pulse arrival time (PAT), pulse transit time (PTT) or pulse wave velocity (PWV) (Catcheside et al., 2002). Furthermore, Catcheside et al. (2002) noted significant changes in PWA after noise-exposure without any visually discernible EEG changes.

Therefore, these results suggest that the PWA and HR could be sensitive sleep disturbance markers to environmental noises, particularly changes in PWA given close relationships with sympathetic nervous system activation underpinning skin vasoconstriction responses that dominate cardiovascular activation and blood pressure responses to transient sensory disturbances in sleep.

2.6 Synthesis and research aims

The macro-structure of sleep does not capture potentially more clinically informative more subtle physiological changes in sleep. Whilst relationships might not be causal, environmental noise such as road traffic noise has been associated with cardiovascular diseases. Therefore, objective measurement of cardiovascular changes such as finger vasoconstriction could be a useful marker of sleep disturbances and adverse health effects due to nocturnal environmental noise exposures as well as a marker of activation of the sympathetic nervous system. Therefore, this thesis focusses on the use of finger PPG recordings to assess pulse wave amplitude (PWA)-drops to assess sleep disturbance in response to environmental noise as well as cardiovascular disturbances in sleep. The aims of the work described in this thesis were to:

- Develop and validate an automated algorithm for detecting PWA-drops (vasoconstriction) in the PPG signal.
- Prospectively investigate the value of PWA-drops for predicting hypertension and cardiovascular events in large general population datasets.
- Investigate sleep disruption by different types of environmental noise to establish if dose-response relationships exist between PWA-drop occurrence and sound pressure level, noise types and sleep stages in which noises occur.

CHAPTER 3 - DEVELOPMENT OF PULSE WAVE AMPLITUDE DROP DETECTION ALGORITHM

3.1 Introduction

This chapter presents the development and validation of a reliable algorithm for automated detection of PWA. Such an algorithm can be used for systematically evaluating vasoconstriction responses over full-night sleep recordings and for exploration of large cohort datasets. Two algorithms were developed based on separate detection principles and their performance was evaluated on a human scored dataset.

3.2 Methodology

The main difference between the algorithms was in evaluating the envelope over the pulse-oximeter photoplethysmogram (PPG) signal, which forms the basis for finding PWA-drops.

3.2.1 Envelope algorithm (Algorithm 1)

The PWA-drop is characterised by a well-defined quick decay from the baseline PPG signal before each drop occurrence, followed by a slow return to baseline, as shown in Figure 6A. The main outcome of the algorithm is PWA-drop area under the curve (AUC). The functioning of the algorithm in more details is as follows

1. The PPG signal is filtered using low-pass 3rd order Butterworth filter with a cut-off frequency at 100 Hz in order to remove extraneous signal noise.

2. The envelope around the filtered PPG signal is determined by an adaptive t_{FPW} second long non-overlapping windows ($w_{1,2,n...N}$) in which the minima and maxima of the signal are found, as shown in Figure 6A.

3. The envelope of the signal, shown in Figure 6B, is then found by interpolating the curve through the minima and maxima points on the finger pulse wave (FPW). The envelope is then smoothed using a 7-point moving average filter.

4. As shown in Figure 6C, the PPG magnitude is derived by subtracting the lower signal envelop from the upper envelope. The FPW magnitude is identical to peak-to-trough distance of the PPG individual peaks.

5. In the last step, the PWA-drops are found and characterised using the PPG magnitude, as illustrated in Figure 6D. The PWA-drop is defined by three points, namely, FPW response start, FPW response end and FPW response minima. These points are found on a point-by-point comparison along the length of the FPW magnitude curve. A PWA-

drop start point, $FPW_{S,n}$, where n indicates an arbitrary position along the curve, satisfies $FPW_n > FPW_{n+1}$. When such a point is found, the FPW response minimal point ($FPW_{M,n}$) can be found as the first point from $FPW_{S,n}$ onwards which satisfies $FPW_n < FPW_{n+1}$. Lastly, the FPW response end-point ($FPW_{E,n}$) is found as the first point from $FPW_{M,n}$ onwards which satisfies $FPW_n > FPW_{n+1}$. After $FPW_{E,n}$ is defined the search continues for the next set of FPW response characteristic points repeatedly until the end of the FPW magnitude signal.

6. For the PWA-drop, characterised by the three points, to be recognised as valid the following conditions had to be satisfied:

    - $FPW_{M,n} \leq 0.9 \times FPW_{S,n}$ (The drop has to be at least 10% lower than the starting point value)
    - $FPW_{E,n} \leq FPW_{S,n}$ (The FPW response end point cannot be bigger than PWA-drop starting point)
    - $FPW_{M,n} \geq 0.1 \times FPW_{S,n}$ (This condition is for removing artefacts such as movement or when the device fell off and the signal was zero)

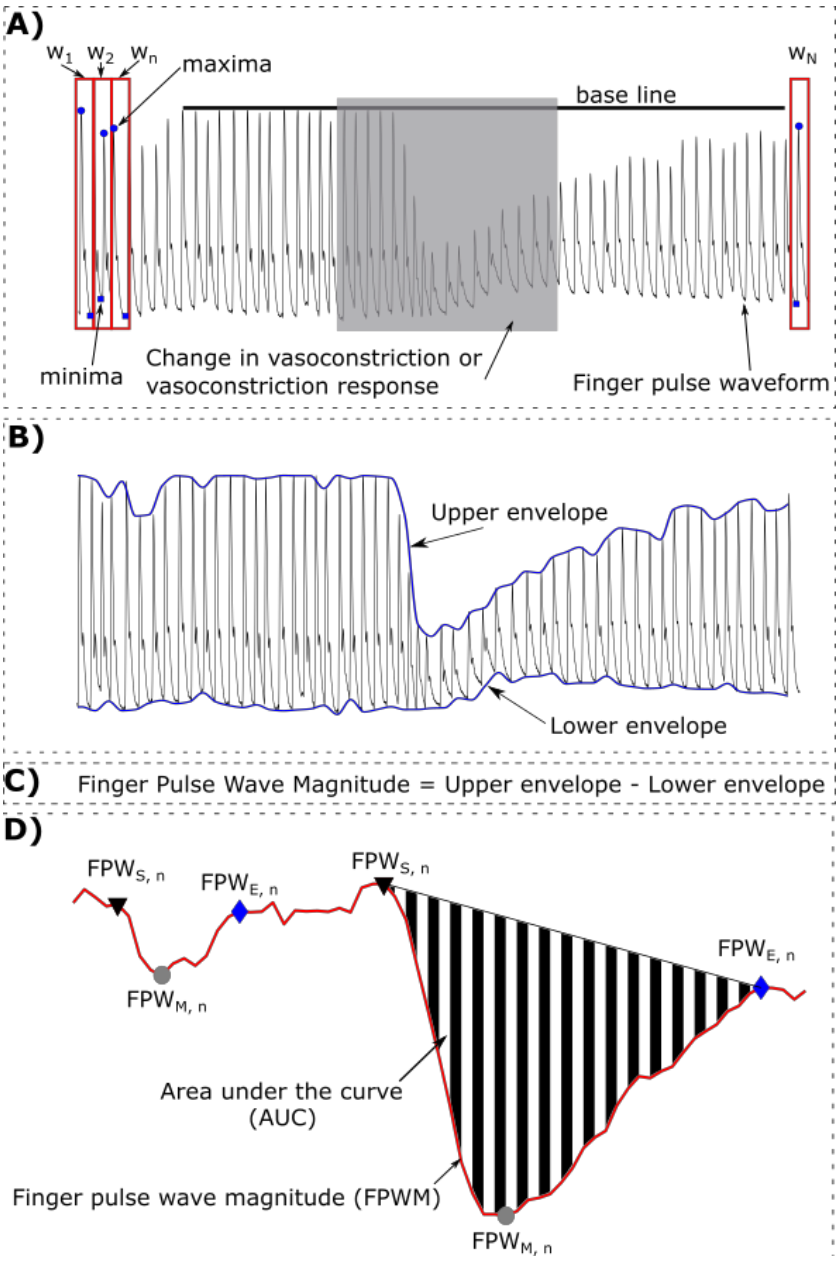

Figure 6: Schematics showing the 4 main stages of the vasoconstrictive response search and characterisation algorithm.

3.2.2 Moving window algorithm (Algorithm 2)

Pre-processing of the signal

The PPG signal is pre-processed to clean and prepare the signal for PWA-drop detections (Figure 7). Raw data were filtered using a Butterworth low-pass filter with a cut-off frequency of 40 Hz, since there is no or minimal physiologically relevant information above that frequency (Binghe and Jinglin, 1998). Then, the first derivative of each signal sample is used to find the peaks and trough points of each pulse waveform (Xu et al., 2007). Finally, a cubic spline was fitted and subtracted from the original signal to remove the floating baseline so that the remaining signal reflects pulsatile amplitude changes above a stationary zero baseline.

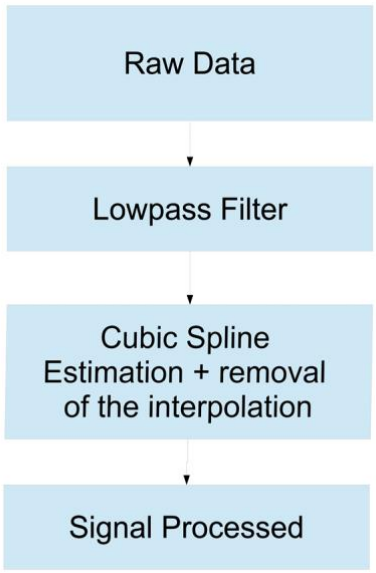

Figure 7: Pre-processing steeps
of the PPG signal.

Algorithm detection (Figure 8)

Two moving average windows were applied to the pre-processed signal to find PWA-drops and determine their size. Each window lasted 7 pulses and measured the mean baseline amplitude and mean decreased amplitude, respectively. As the amplitude of the PWA signal can vary rapidly, the 7 pulse windows were found to allow for detection of changes in the fast varying PWA-signal yet rejecting the non PWA-signal changes. The ratio between the mean baseline amplitude and mean decreased amplitude formed the amplitude ratio where PWA-drop was identified if the amplitude ratio was $\leq$ 75%.

This threshold was shown to demonstrate the most consistent performance in terms of F1-score, as shown in a sensitivity analysis presented in Figure A-1 and Figure A-2. Another crucial ratio was the ratio between the end of the PWA-drop and baseline which had to be $\geq$ 80% for a valid PWA-drop. This cut-off criteria was chosen according visual inspection of PWA-drops.

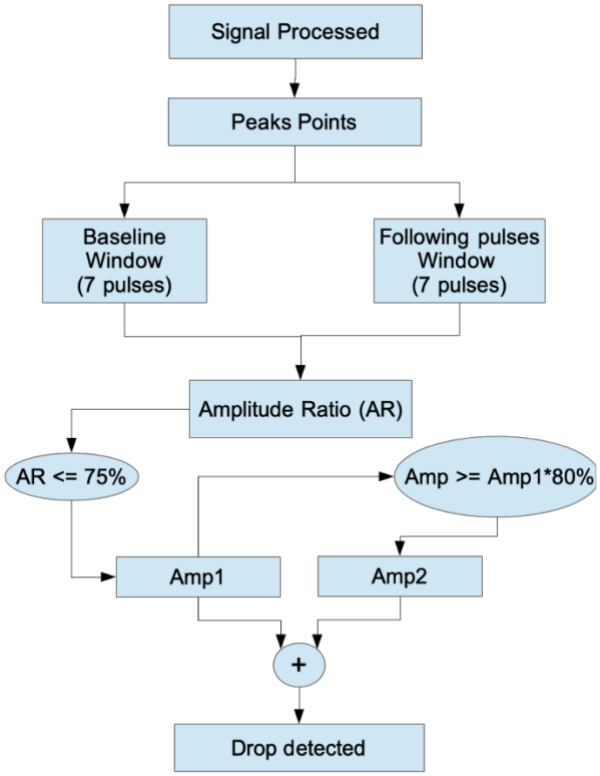

Figure 8: Algorithm 2 flow chart.

So detected PWA-drops where then characterised in terms of their length and area under the curve (see Figure 10) which was calculated as follows:

$$AUC = \left(\frac{Area\ Max\ drop - Area\ drop}{Mean\ MBA}\right) * 100, \qquad (1)$$

where Area Max drop and Area drop are defined in Figure 9, and Mean MBA is the mean amplitude baseline.

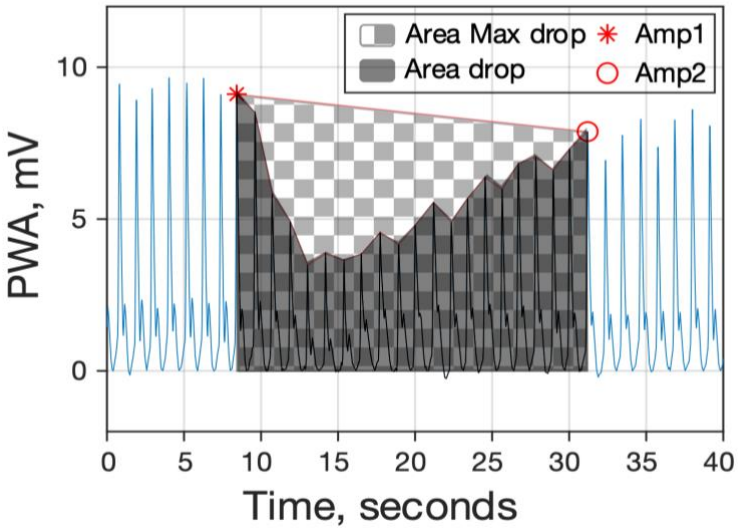

Figure 9: Description of Area Max drop and Area drop.

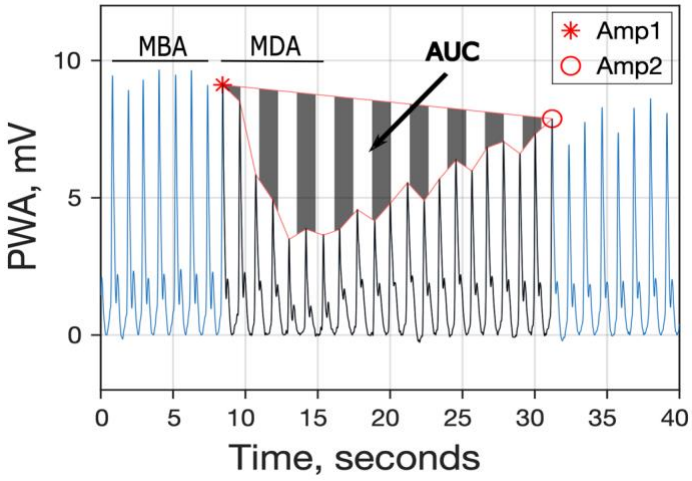

Figure 10: Parameters of one detected PWA drop by the algorithm.

3.2.3 Validation of the algorithms in a clinical dataset

PSG recordings and manual scoring

Both algorithms were validated on the PPG-data extracted from PSG overnight recordings of 16 patients (mean ± SD age 50.9 ± 6.3 years, 13 females) randomly sampled from the HypnoLaus Sleep Cohort database, Switzerland (Heinzer et al., 2015). This scored PPG dataset was scored by two scorers who visually inspect the signals and identified PWA drops where a minimal 30% reduction in the signal was observed. A “consensus” dataset was created from both scorers to evaluate the performance of each algorithm.

Comparison of scorers and algorithms

The degree of agreement between scorers was assessed via percentage overlap (%) (Equation 2); where perfect agreement would have a 100% overlap and complete disagreement 0% overlap (Figure 11).

$$\text{Percentage overlap} = \left(\frac{Intersection}{Union}\right) * 100, \qquad (2)$$

where Intersection is the overlap length between the PWA-drops as shown in Figure 11, and Union is the total length of both PWA-drops as shown in Figure 11.

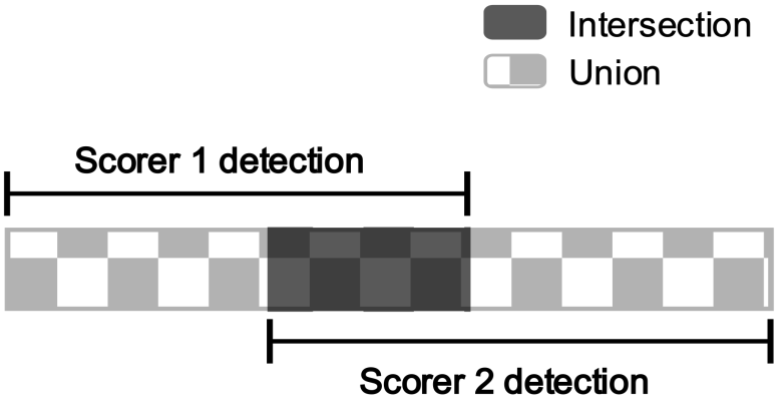

Figure 11: Description of percentage overlap.

Algorithm performance was assessed using a contingency table which was constructed by calculating the number of true positive (TP), false positive (FP) and false negative (FN). A TP was defined if a PWA-drop detected by an algorithm which overlapped with scorers' detection for at least the percentage overlap (0 to 100%). Subsequently, any drops that did not meet these criteria were considered as an FN (if missed) or an FP (if detected by an algorithm but not scored by scorers). This overlapping analysis rewards PWA-drops detected that align perfectly with the other human scoring. As PWA-drops are relatively rare, the number of true negative (TN), used generally for the computation of specificity, was not calculated. In this case, the total length of data not determined as PWA-drops by either scorer would be defined as TN and then provide a bias specificity (Yetton et al., 2016, Warby et al., 2014). The algorithm performance was ultimately evaluated using F1-score which is based on recall and precision measures:

$$Recall = \frac{TP}{TP + FN} = fraction\ of\ true\ PWA\ drops\ detected/scored \quad (3)$$

$$Precision = \frac{TP}{TP + FP} = fraction\ of\ detections\ that\ are\ correct \quad (4)$$

From these two measures, the F1-score was computed as follows:

$$F_1 = 2 * (\frac{recall * precision}{recall + precision}) \quad (5)$$

The F1-score ranges from 0, representing random, and 1, representing perfect classification. The grand average score was obtained by the arithmetic mean of the F1-scores of all participants.

The inter-scorer agreement was also assessed via the F1 score. This was done by evaluating the degree of agreement between the scorers, measured in percentage overlap (see Equation 2 and Figure 11), with respect to only one of the scorer's ratings which were treated as "gold standard" or absolute truth. Treating one scorer rating as being correct, allowed the formation of contingency tables and then on calculation of F1 score. This also provided an indication of the optimal percentage overlap between the scorers for declaring valid PWA-drops.

3.3 Results

3.3.1 Algorithms and human scorer PWA-drop detection

Figure 12 shows a comparison of both scorers' detection. The threshold was chosen at 20% when both macro-averaged F1-score curves (= 0.66) started to decrease, indicating that the detection of both scorers started to differ.

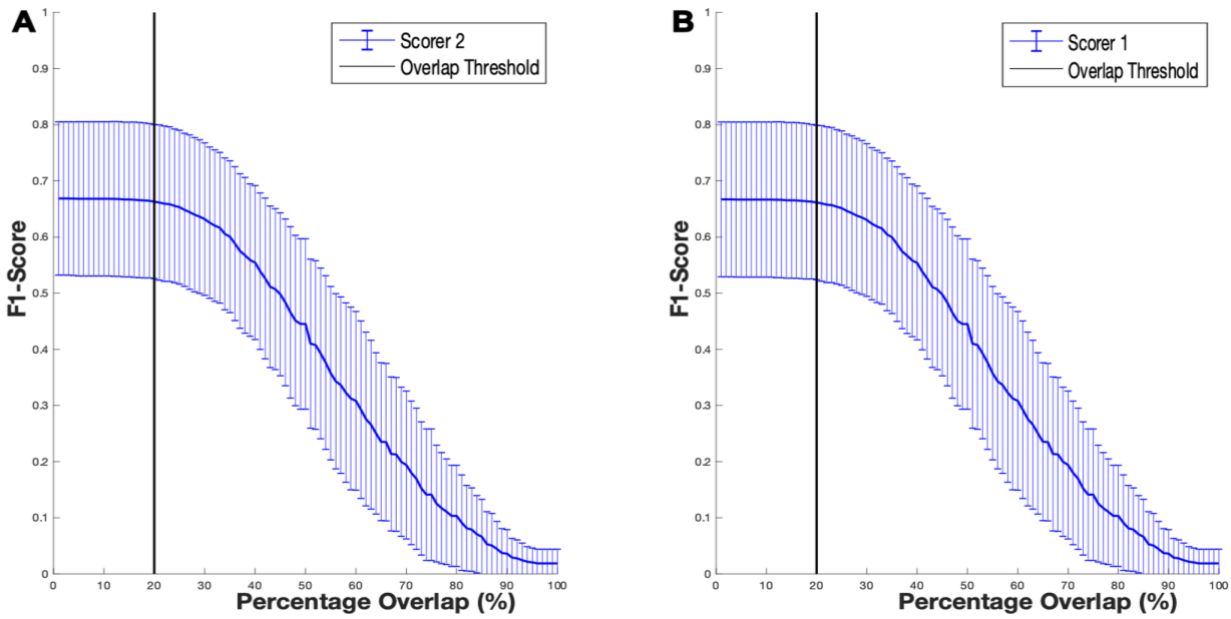

Figure 12: The F1-score curves with standard deviation as a function of the percentage overlap (%). To construct each curve the scorer' scorings were compared in A) with Scorer 2 as reference, and in B) with Scorer 1 as reference. Values are mean ± SD.

Table 1: Summary PWA-drop detection by both algorithms and human scorers for all overnight recordings.

Participants	Scorer 1	Scorer 2	Scorer consensus	All scoring	Envelope algorithm	Moving window algorithm
1	396	81	80	397	217	150
2	29	25	18	36	40	19
3	109	92	66	136	219	159
4	89	95	59	125	218	88
5	224	226	185	267	296	268
6	287	139	111	315	392	340
7	241	231	212	261	285	225
8	414	231	229	423	453	375
9	127	297	118	306	359	259
10	89	87	62	114	227	147
11	255	321	234	342	352	251
12	346	379	338	583	532	505
13	69	105	48	126	293	204
14	186	335	167	354	278	243
15	146	228	132	241	197	154
Total	3007	3068	2059	4027	4358	3387

The number of PWA-drops detected are shown in Table 1 for the all overnight recordings (lights “on” to lights “off”). Agreement between scorers is declared at 20% overlap threshold, the threshold being optimal at 20%.

Scorer 2 generally detected longer arousals than Scorer 1, the mean length of all arousals during all the sleep recordings were 9.0±5.3 s and 15.9±7.8 s for Scorers 1 and 2, respectively.

3.3.2 Algorithm performance

A consensus dataset was created with 20% overlap as a minimum to determine an agreement between scorers. The moving window algorithm (Algorithm 2) seemed to perform slightly better overall for all overnight recordings at an overlap of 20% than the envelope algorithm (Algorithm 1) (Figure 13). Nonetheless, standard deviations of both algorithms crossed between 0% and 20% in all cases.

The fraction of all detections from the moving window algorithm that were correct (Precision) for 20% overlap was systematically higher than the envelope algorithm (Table A-1). However, the fraction of true PWA-drops the moving window algorithm detected (Recall) was systematically lower than the envelope algorithm in all cases (Table A-1). Therefore, the moving window algorithm detected fewer false negatives and more false positives than the envelope algorithm. Nevertheless, the standard deviations of precision and recall for both algorithms systematically crossed at 20% overlap. The average length of the PWA-drops detected by the envelope algorithm and the moving window algorithm were 31.6±18.0 s and 19.5±8.3 s, respectively. In comparison, the average lengths of the consensus PWA-drops scoring were 13.5±5.9 s and 12.1±6.2 s for the agreement between scorers and for the overall scoring, respectively.

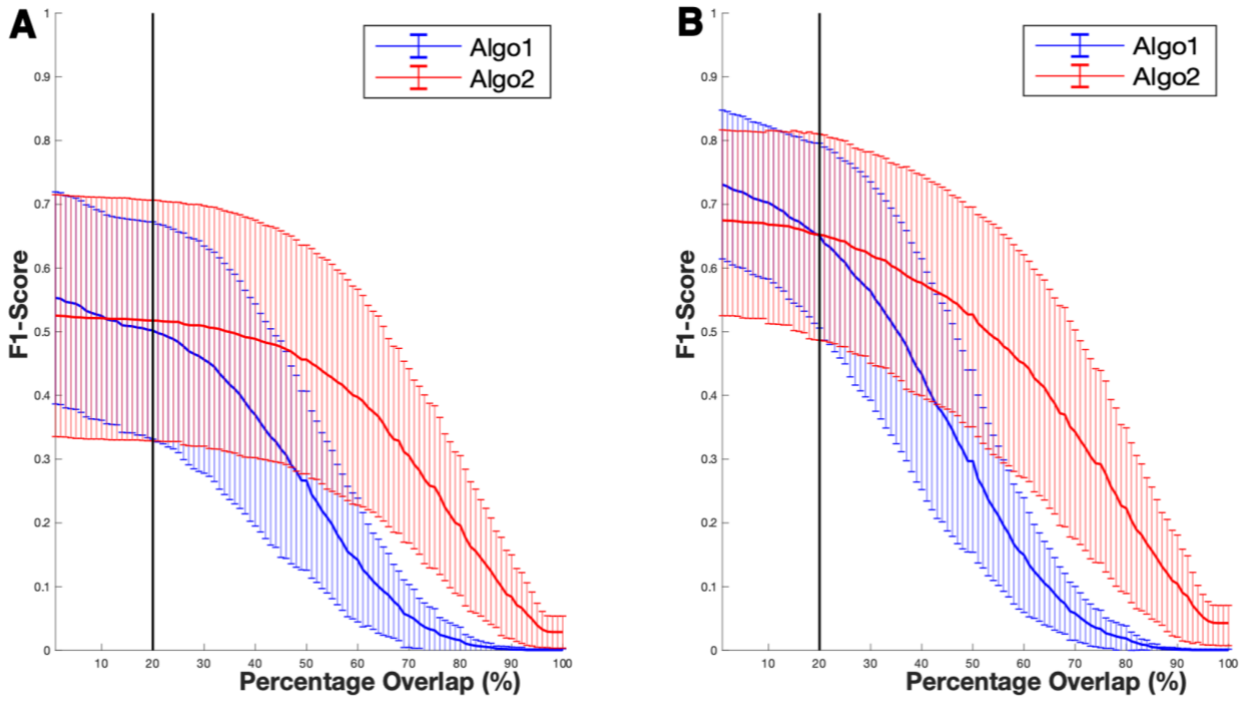

Figure 13: The F1-score curves with standard deviation as a function of percentage overlap (%) during all sleep recordings. A) the "consensus" scoring agreement between scorers was the reference to construct the curves of both algorithms, and B) all scored PWA-drops of both scorers was the reference to construct the curves of both algorithms. Algorithm 1 is the envelope algorithm; Algorithm 2 is the moving window algorithm. Values are mean ± SD.

3.4 Discussion

This study developed two algorithms for automated detection of finger pulse wave amplitude (PWA)-drops and compared them against human scored data.

To best define the detection of a PWA-drop, the results from two expert human scorers were compared. The percentage overlap corresponding to the best agreement between scorers was determined by plotting the average F1-score curves between the two scorers as a function of percentage overlap. A percentage overlap threshold of 20% was chosen in this study as the mean of the F1-score curves was unchanged until 20% overlap. After 20% overlap the difference between the two mean F1-score curves starts to decrease. The two human scorings were then used as a gold standard to assess the performance of both PWA-drop detection algorithms. Betta et al. (2020) have already used this dataset for validation and chose a percentage overlap of at least 10% which is relatively low, 10% of the mean length arousals for Scorer 1 = 0.9±0.5 s and Scorer 2 = 1.5±0.7 s for all overnight recordings. Moreover, the same percentage overlap was applied for each scorer, despite the differences in the lengths of the scored PWA-drops for Scorer 1 and Scorer 2. The approach described in this chapter instead considered the union between

the scored and algorithm-detected PWA-drops as well as a “consensus” dataset. The percentage overlap in this study was also chosen using a novel and robust approach that considered the F1-score rather than an arbitrary choice.

The moving window algorithm seems to perform slightly better than the envelope algorithm when compared to the two expert scorers with 20% overlap. This difference might be due to a lower amplitude threshold in the envelope algorithm which would find more false positives (detected by the algorithm but not by the scorer) than the moving window algorithm. It could also be explained by somewhat different algorithm approaches, where the envelope algorithm uses the envelope of the signal to determine the amplitude of a drop and the moving window algorithm uses the peak amplitudes of each pulse in the windows to calculate the amplitude ratio used for PWA-drop detection.

PWA-drop detection still relies largely upon human scoring which suffers from variable intra- and inter-scorer agreement. It is also a time-consuming process, making it impractical for use on large datasets.

Transient pulse wave amplitude reductions as a marker of autonomic activation is potentially more useful for identifying physiological disturbances during sleep than conventional EEG approaches. Therefore, a PWA-drop algorithm could be very useful for automatically detecting cardiovascular reactions to various stimuli or symptoms of cardiovascular disease to help advance evidence-based clinical practice and further research into sleep disturbance mechanisms and outcomes.

CHAPTER 4 – ASSOCIATIONS BETWEEN CARDIOVASCULAR PATHOPHYSIOLOGY AND PULSE WAVE AMPLITUDE DROPS DURING SLEEP

4.1 Introduction

The aim of this chapter is to present the exploration of two cohort datasets in terms of the association between PWA-drop based metrics and cardiovascular endpoints. We hypothesised that PWA-drop based markers would be predictive of hypertension and cardiovascular events. One of the datasets has already been analysed by Hirotsu et al. (2020) using a different detection algorithm and thus this analysis was also designed to serve as a cross validation of PWA-drop approaches more generally using an independent but similar algorithm approach.

4.2 Methodology

4.2.1 Study design and participants

Two population-based studies were used in this investigation, the Men Androgen Inflammation Lifestyle Environment and Stress (MAILES) (Grant et al., 2014) and the HypnoLaus Sleep cohort study (Heinzer et al., 2015).

MAILES cohort

The MAILES was a cohort study to assess the association of sex steroids, inflammation, environmental and psychosocial factors with cardio-metabolic disease risk in men (Grant et al., 2014). This cohort was created by harmonising two studies: the Florey Adelaide Male Ageing Study (FAMAS) and eligible (at least 35 years old) male participants of the North West Adelaide Health Study (NWAHS). Two clinical assessments occurred in 2002-06 (n=2563) and 2007-10 (n=2038). In 2010, MAILES participants completed a CATI survey (n = 1,629). Of these participants, 184 responded “yes” to “Have you ever been diagnosed with obstructive sleep apnoea with a sleep study?” and 1,445 men responding “no” were invited to undergo a sleep study, with 75.2% agreeing (Appleton et al., 2016). The home-based polysomnography sub-study (Embletta X100, Embla Systems) was conducted in 2010 and 2011 with 837 completed successful studies, and 752 had finger oximetry recorded. Finally, after artefacts exclusion (e.g. ectopic beats, probe off, movement artefacts, hypnogram issues) 738 valid studies were included in this analysis. The polysomnography recording included measures of electroencephalogram (EEG), electrooculogram (EOG), electromyography (EMG), nasal pressure, thoracic and abdominal efforts, oximetry, and body position. One experienced sleep technician performed manual scoring of all PSGs according to the 2007 American Academy of Sleep Medicine (AASM) alternative criteria (Iber et al., 2007).

HypnoLaus cohort

Participants from the population based CoLaus/PsyCoLaus cohort study in Lausanne, Switzerland were invited to take part in the HypnoLaus Sleep cohort study (Heinzer et al., 2015). HypnoLaus was a cohort study to investigate the prevalence of sleep-disordered breathing in the general population. Participants had biomedical clinic assessments and were equipped with a PSG recorder (Titanium, Embla Flaga, Reykjavik, Iceland). All sleep recordings were home-based with a total of 2162 participants with 2146 valid studies including EEG, EOG, EMG, electrocardiogram (ECG), airflow (nasal cannula), thoracic and abdominal efforts, snoring, body position, oxygen saturation (SpO_2), and oximetry (Hirotsu et al., 2020). Two experienced sleep technicians performed manual scoring of all PSGs according to 2007 American Academy of Sleep Medicine (AASM) alternative criteria (Iber et al., 2007).

Cohort outcomes

In both studies, apnoeas were defined as complete cessations of airflow, measured using nasal cannula pressure, lasting ≥ 10 s and hypopnea as > 50% decrease in nasal pressure (or in both thoracic and abdominal excursions) with an associated ≥ 3% oxygen desaturation or an EEG arousal (Iber et al., 2007). The apnoea hypopnea index was defined as the number of apnoea and hypopneas per hour of sleep. In both cohorts, diabetes was defined when fasting plasma glucose levels were ≥ 7.0 mmol/L or diabetic medication use, and hypertension was defined as systolic blood pressure ≥ 140 mmHg and/or diastolic blood pressure ≥ 90 mmHg, and/or use of anti-hypertensive medication.

4.2.2 Detection of pulse wave amplitude (PWA)-drops

PWA-drops were identified using the moving window algorithm described in Chapter 3 when the amplitude ratio was ≤ 75%. Mean PWA-drop duration and area under the curve (AUC) and PWA-drop index were then estimated. The PWA-drop index is the total number of PWA-drops during sleep divided by the total sleep time.

4.2.3 Covariates

Questionnaire and physical examination were used at the time of the polysomnography study to determine age, sex, and body mass index (BMI). Smoking status (non-smoker, former smoker and current smoker) and alcohol consumption (number of drinks per week) were also assessed at the time of the PSG study for the HypnoLaus cohort. However, the MAILES cohort recorded smoking status and alcohol consumption anytime during the 4 years leading up to the PSG study. Total sleep time, AHI, number of PWA-drops, diabetes and, in the case of cardiovascular events, hypertension were also included as potential confounders.

4.2.4 Outcome assessment

Hypertension and previous cardiovascular (CV) events were the outcomes of interest. A previous CV event was defined as a doctor diagnosed myocardial infarction, stroke or acute coronary syndrome. Systolic blood pressure, diastolic blood pressure and cardiovascular events were assessed at the time of the PSG study in HypnoLaus, and within the 4 years preceding the PSG study in MAILES.

4.2.5 Statistical analysis

Multivariate-adjusted logistic regression analysis was used to identify associations between prevalent hypertension or cardiovascular events (dependent variables) and PWA-drop features (mean AUC, mean duration and PWA-drop index) (independent variables). Associations between cardiovascular events and PWA-drop features were assessed individually in separate models. In total 6 models were performed. Confounders (age, sex, BMI, smoking status, AHI, total sleep time, alcohol consumption) were identified based on previous literature (Hirotsu et al., 2020) and were included in all models. When testing the PWA-drop mean AUC and mean duration, models were additionally adjusted for the number of PWA-drops due to an inverse correlation between them, to maintain comparability with previous work (Hirotsu et al., 2020). Associations between PWA-drop features and cardiovascular events were furthermore adjusted for diabetes and hypertension.

PWA-drop features were treated as continuous variables and were tested for non-linearity using restricted cubic splines in the “rms” R package. For linear associations, the findings were summarised using quartiles of the PWA-drop features for comparison with previously published associations. Each model was assessed in both cohorts (HypnoLaus and MAILES) separately and combined.

Interactions between PWA-drop features and sex were also performed since MAILES was a male only cohort whilst HypnoLaus included both males and females. Interactions between PWA-drop features and apnoea hypopnea index were also examined as OSA has been found to be associated with PWA-drop occurrence (Schnall et al., 1999). Moreover, interactions between PWA-features and the studies on the pooled dataset were also examined. Multi-collinearity among independent variables was avoided using a variance inflation factor (VIF) < 5 through linear regression analysis. Influences of outliers were assessed graphically using the model residual distribution. Predictive performance of the model was assessed using the Harrell’s C-index (area under the ROC curve) and Somers’ Dxy indices corrected for optimism using bootstrapping (Newson, 2010). The models were compared to a model containing only the confounder variables using a likelihood ratio test. Results are expressed as odds ratios (ORs) with 95% confidence intervals (CIs). Null hypotheses were rejected when $p < 0.05$.

4.3 Results

4.3.1 Baseline characteristics

The combined cohort dataset had 2914 participants; 2162 from HypnoLaus cohort and 752 from MAILES cohort, where 30 (1.0%) participants were excluded due to missing hypnogram data and/or insufficient PWA signal quality. The MAILES cohort had higher mean age, BMI, alcohol consumption, total sleep time, AHI and a lower percentage of non-smokers, as shown in Table 2. The proportion of diabetic participants were similar in both cohorts. 44% (n = 1277) and 6% (n = 180) of the pooled dataset had hypertension and a CV event, respectively. The proportion of participants with hypertension and CV events was higher in the MAILES cohort. Additionally, a total of 23 (0.8 %) and 144 (5.0%) participants had missing data on the hypertension and CV event, respectively.

Table 2: Baseline characteristics of study participants.

	HypnoLaus (N=2146)	**MAILES (N=738)**	**Total (N=2884)**
Sex			
Male	N = 1050 (49%)	N = 738 (100%)	N = 1788 (62%)
Female	N = 1096 (51%)	N = 0 (0%)	N = 1096 (38%)
Age (years)			
Mean (SD)	59 (11)	61 (11)	59 (11)
BMI (kg/m^2)			
Mean (SD)	26 (4.4)	29 (4.1)	27 (4.4)
Missing	N = 13 (0.6%)	N = 0 (0%)	N = 13 (0.5%)
Alcohol consumption (numbers of drink per week)			
Mean (SD)	6.5 (7.9)	8.2 (11)	7.0 (8.8)
Missing	N = 0 (0%)	N = 1 (0.1%)	N = 1 (0.0%)
Smoking status			
Never	N = 878 (41%)	N = 269 (36%)	N = 1147 (40%)
Current	N = 395 (18%)	N = 112 (15%)	N = 507 (18%)
Former	N = 850 (40%)	N = 342 (46%)	N = 1192 (41%)
Missing	N = 23 (1.1%)	N = 15 (2.0%)	N = 38 (1.3%)
Total sleep time (hours)			
Mean (SD)	6.7 (1.2)	7.7 (1.3)	6.9 (1.3)
Missing	N = 0 (0%)	N = 10 (1.4%)	N = 10 (0.3%)
AHI (events/hour)			
Mean (SD)	9.1 (13)	15 (14)	11 (13)
Missing	N = 0 (0%)	N = 1 (0.1%)	N = 1 (0.0%)

	HypnoLaus (N=2146)	MAILES (N=738)	Total (N=2884)
Number of PWA-drops (Asleep)			
Mean (SD)	250 (120)	190 (100)	230 (120)
PWA-drop mean AUC (%s)			
Mean (SD)	650 (110)	600 (85)	640 (110)
PWA-drop mean Duration (s)			
Mean (SD)	22 (2.9)	21 (2.6)	22 (2.8)
PWA-drop mean Index (events/hour)			
Mean (SD)	37 (16)	30 (15)	35 (16)
Hypertension			
No	N = 1259 (59%)	N = 326 (44%)	N = 1584 (55%)
Yes	N = 886 (41%)	N = 391 (53%)	N = 1277 (44%)
Missing	N = 2 (0.1%)	N = 21 (2.8%)	N = 23 (0.8%)
Diabetes			
No	N = 1933 (90%)	N = 651 (88%)	N = 2584 (90%)
Yes	N = 211 (10%)	N = 69 (9%)	N = 280 (10%)
Missing	N = 2 (0.1%)	N = 18 (2.4%)	N = 20 (0.7%)
CV event			
No	N = 1928 (90%)	N = 632 (86%)	N = 2560 (89%)
Yes	N = 88 (4%)	N = 92 (12%)	N = 180 (6%)
Missing	N = 130 (6.1%)	N = 14 (1.9%)	N = 144 (5.0%)

The distribution of PWA-drop features during sleep for both cohorts is shown in Figure 14. On average, 35±16 PWA-drops occur per hour with a mean AUC of 640±110 %s and a mean duration of 22±2.8 s. The mean number of PWA-drops was higher in HypnoLaus (250) than MAILES (190) however the standard deviation was higher in the HypnoLaus cohort.

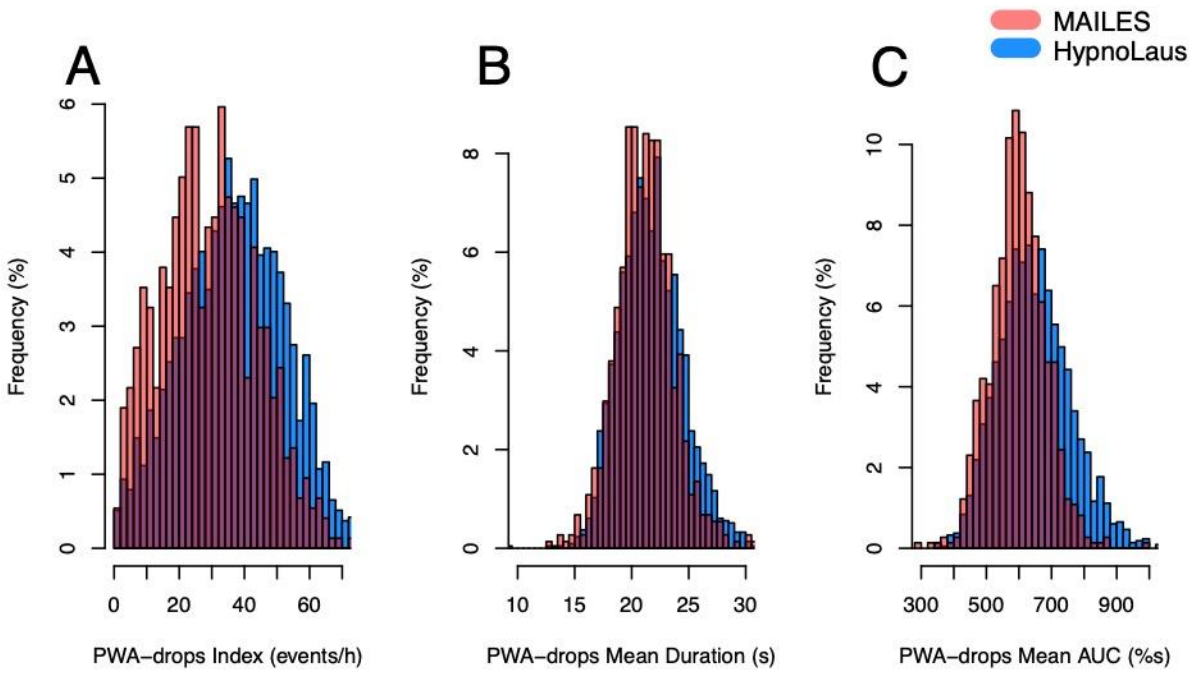

Figure 14: Histograms showing the distribution of PWA-drop features during sleep for both cohorts. A) PWA-drop index B) PWA-drop mean duration C) PWA-drop mean AUC.

4.3.2 Pulse wave amplitude drops and prevalence of hypertension

A higher AUC of PWA-drops was significantly associated with 84% increased odds of prevalent hypertension in the MAILES cohort (Quartile 4 vs Quartile 1: 1.84 (1.10-3.08)) (Figure 15B and Figure 15E) and 42%, HypnoLaus cohort (Q4 vs Q1: 1.42 (1.03-1.96)) (Figure 15A and Figure 15D) and 58% in pooled dataset (Q4 vs Q1: 1.58 (1.21-2.07)) (Figure 15C and Figure 15F), as well as in linear increase of odds ratio ($p = 0.031$, $p = 0.009$ and $p = 0.001$ respectively).

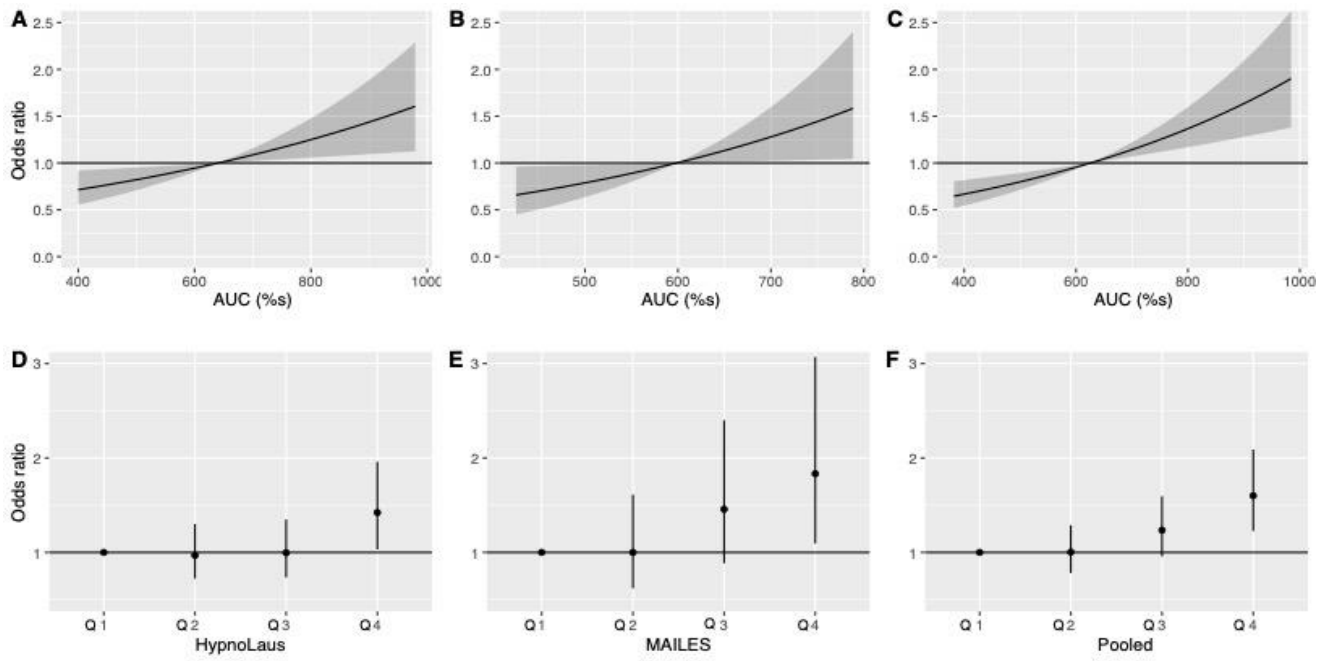

Figure 15: PWA-drop mean AUC and hypertension. Linear (A-C) and quartiles (D-F) odds ratios with 95% confidence intervals.

The highest quartile (Q4 vs Q1: 1.29 (1.01-1.66)) for the PWA-drop mean duration in participants from pooled datasets was statistically significant (Figure 16C, Figure 16F and Table B-4) as well as linearly (p = 0.005 and see in Table B-6) suggesting an increased odds of hypertension for longer PWA-drops.

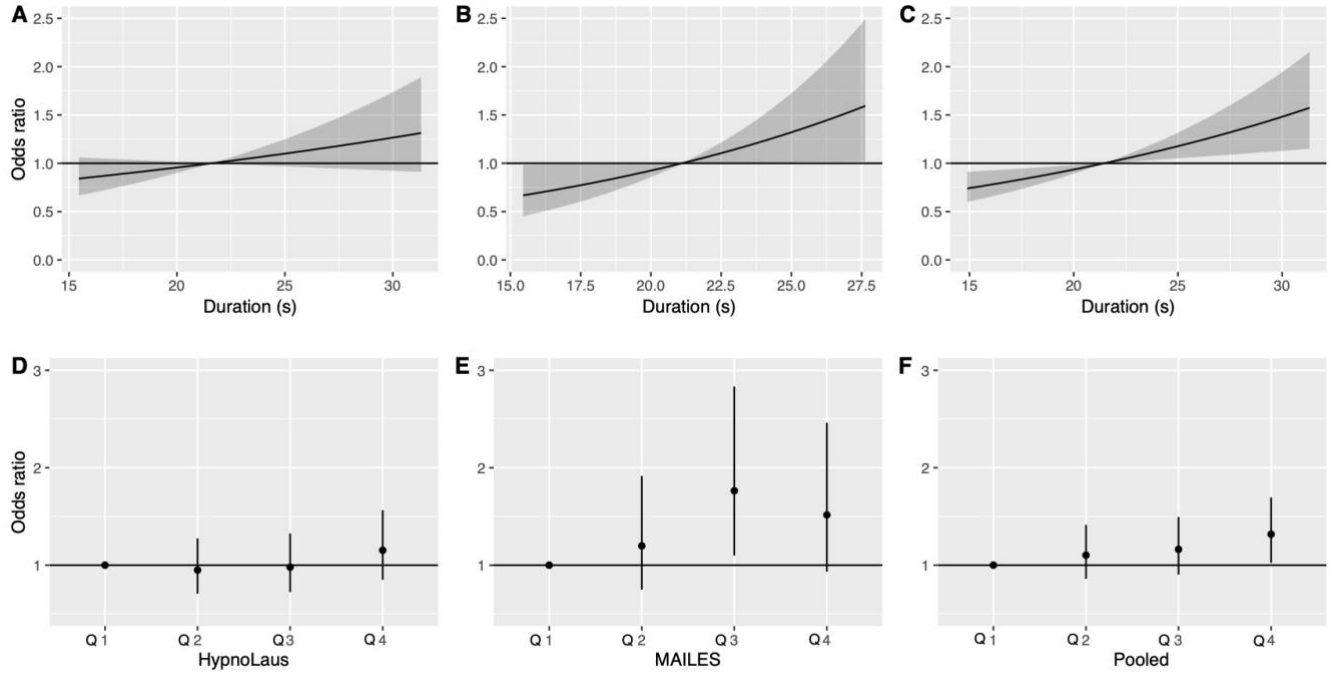

Figure 16: PWA-drop mean duration and hypertension. Linear (A-C) and quartiles (D-F) odds ratios with 95% confidence intervals.

The linear prediction of prevalent hypertension in the HypnoLaus cohort was not significantly associated with the PWA-drop mean index (p = 0.082 and see Table B-6), however the highest quartile in the HypnoLaus cohort was statistically significant (Q4 vs Q1: 0.65 (0.48-0.86)) (Figure 17A, Figure 17D and Table B-4).

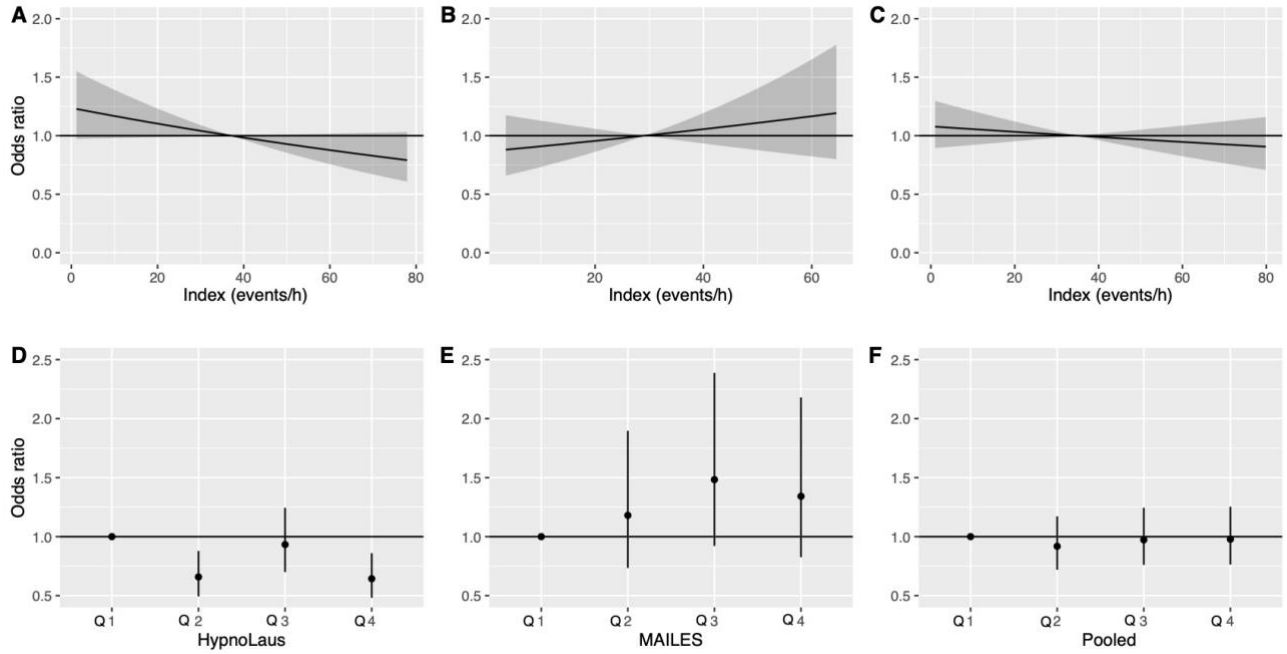

Figure 17: PWA-drop mean index and hypertension. Linear (A-C) and quartiles (D-F) odds ratios with 95% confidence intervals.

In the HypnoLaus cohort, the PWA-drop mean AUC association with hypertension prevalence was found using the moving window algorithm developed in Chapter 2 and the algorithm from Hirotsu et al. (2020) as shown in Table 3. However, PWA-drop mean duration and index were only significantly associated with hypertension using the algorithm from Hirotsu et al. (2020).

Table 3: Algorithm comparison in terms of PWA-drop features and hypertension prevalence in the HypnoLaus cohort. Odds ratio with 95% confidence intervals.

Hypertension prevalence	**Moving window algorithm**	**Hirotsu et al. (2020) algorithm**
	OR [95% CI]	OR [95% CI]
PWA-drop index (10 events/h decrease)	1.06 [0.99-1.13]	1.06 [1.01-1.12]
PWA-drop mean duration (1 s increase)	1.03 [0.99-1.07]	1.06 [1.02-1.10]
PWA-drop mean AUC (10 %s increase)	1.01 [1.01-1.03]	1.01 [1.01-1.02]

The likelihood ratio test between models with and without PWA-drop features (Table 4) suggests that the mean AUC and mean duration are two factors that improve predictive performance of the model in the pooled dataset. However, there is a lack of consistency in the results between MAILES and HypnoLaus.

Table 4: Likelihood ratio test with and without PWA-drop features included in the models with hypertension prevalence.

Hypertension prevalence	HypnoLaus	MAILES	Pooled
PWA-drop mean AUC	χ^2 = 6.85, p = 0.009	χ^2 = 4.85, p = 0.028	χ^2 = 14.00, p < 0.001
PWA-drop mean duration	χ^2 = 2.14, p = 0.144	χ^2 = 3.47, p = 0.062	χ^2 = 7.14, p = 0.008
PWA-drop index	χ^2 = 2.90, p = 0.088	χ^2 = 0.44, p = 0.506	χ^2 = 0.93, p = 0.335

4.3.3 Pulse wave amplitude drops and previous cardiovascular events

Participants with a lower PWA-drop index showed a decrease in odds ratio associated with CV event prevalence in the HypnoLaus study (Q4 vs Q1: 0.40 (0.20-0.81)) (Figure 18A, Figure 18D and Table B-5) although the linear association was not significant (p = 0.058 and see Table B-6). However, in the pooled dataset (Q4 vs Q1: 0.73 (0.46-1.17)) and MAILES cohort (Q4 vs Q1: 1.56 (0.77-3.19)) no association was observed between PWA-drop index and CV event prevalence and there were also no linear associations (p = 0.336 and p = 0.066 respectively).

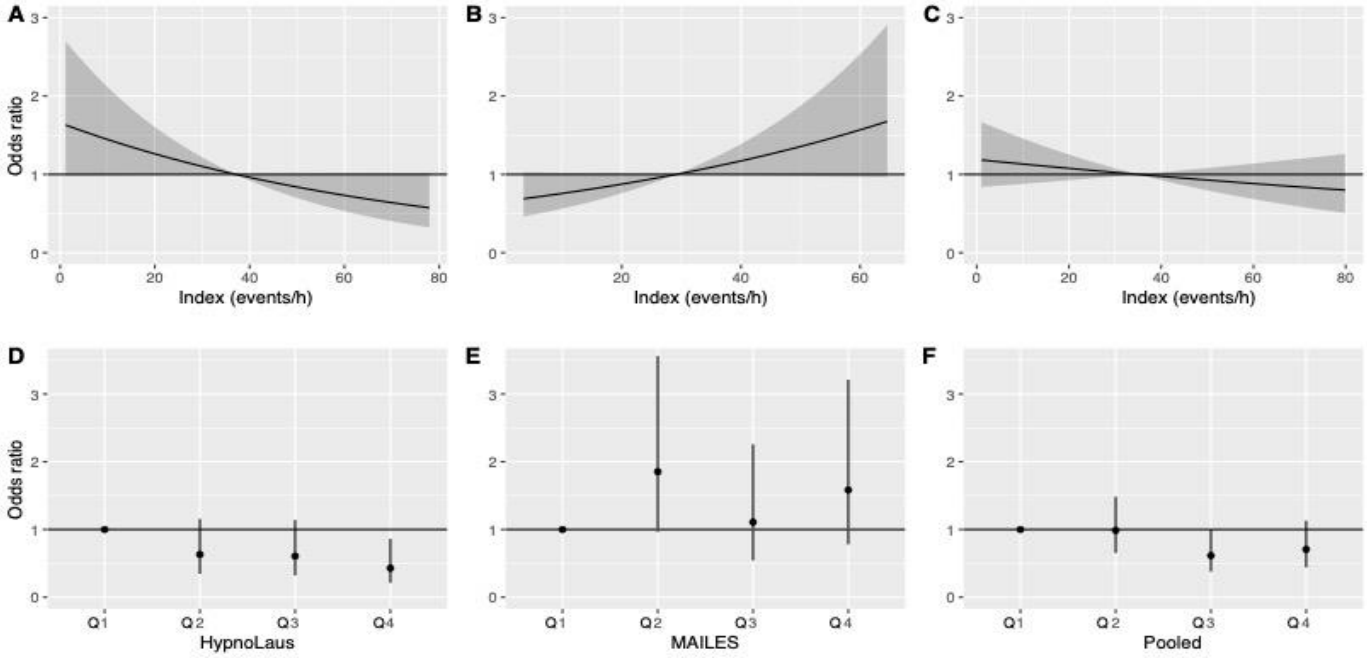

Figure 18: PWA-drop mean index and CV events. Linear (A-C) and quartiles (D-F) odds ratios with 95% confidence intervals.

In the HypnoLaus cohort, the PWA-drop index was associated with cardiovascular events only with the algorithm from Hirotsu et al. (2020) as shown in Table 5.

Table 5: Algorithm comparison in terms of PWA-drop features and CV events in the HypnoLaus cohort. Odds ratio with 95% confidence intervals.

Previous cardiovascular events	**Moving Window algorithm**	**Hirotsu et al. (2020) algorithm**
	OR [95% CI]	OR [95% CI]
PWA-drop index (10 events/h decrease)	1.15 [0.99-1.32]	1.11 [1.00-1.25]
PWA-drop mean duration (1 s increase)	1.01 [0.94-1.09]	1.05 [0.97-1.13]
PWA-drop mean AUC (10 %s increase)	1.01 [0.99-1.03]	1.01 [1.00-1.03]

No significant association was observed between CV events and mean duration and mean AUC (see Figure B-1 and Figure B-2) and none of the PWA-drop features significantly improved the model performance (see Table B-1).

4.3.4 Model validation and specification

All model associations between hypertension prevalence and PWA-drop features (see Table B-2), were validated with all optimism (O) $\leq$ 1% and specified all C-index $\geq$ 0.79 and all Dxy $\geq$ 0.58 for the pooled dataset. Predictive performance for cardiovascular events and hypertension prevalence was similar (Table B-3) with all optimism (O) = 3% and specified all C-index $\geq$ 0.81 and all Dxy $\geq$ 0.62 for the pooled dataset.

4.4 Discussion

This chapter investigated the association between hypertension, CV event prevalence and multiple PWA-drop features. The results suggest that the PWA-drop mean AUC could be a reliable predictor for hypertension independent of total sleep time, apnoea hypopnea index and other clinical and life-style related covariates.

Hirotsu et al. (2020) used another PWA-drop detection algorithm to analyse the data from the HypnoLaus cohort and found significant associations between hypertension prevalence and PWA-drop mean AUC, mean duration and PWA-drop index. In this study using a different algorithm, only the PWA-drop mean AUC was significantly and consistently associated with hypertension prevalence. Since there is no “scorer consensus” on the PWA-drop definition there is inevitably some uncertainty surrounding algorithm performance. However, both algorithms showed the same general trends towards associations of PWA-drop mean AUC with

hypertension prevalence in the HypnoLaus dataset. The algorithm used in this thesis also showed these trends independently in the MAILES dataset, although with overall smaller effect sizes which could be due to lower numbers of cardiovascular events and demographic differences (in BMI and gender). However, a significant association between PWA-drop AUC and hypertension prevalence independent of which algorithm is used, supports that PWA-drops are a useful risk marker of hypertension. This finding is in accordance with previous knowledge relating sympathetic activity with hypertension (Timio et al., 1997).

No association was observed between CV event prevalence and PWA-drop mean AUC and PWA-drop mean duration. The PWA-drop index was associated with CV event prevalence in the HypnoLaus cohort only. Surprisingly, an opposite trend was observed in the MAILES cohort although this was not statistically significant. This could reflect population differences between cohorts (e.g. gender, BMI, alcohol consumption and apnoea hypopnea index). The PWA-drop index has previously been shown to be a predictor of cardiovascular risk (Sommermeyer et al., 2014) where a lower PWA-drop index (evaluated per hour) was associated with lower cardiovascular risk in a cohort of 520 participants from northern Europe. Furthermore, patients with previous CV events generally tend to get treated to prevent another event that could lead to death, which might be the reason why no association was found between PWA-drop features and CV event prevalence. In comparison, patients with hypertension do not get treated systematically because hypertension is not as related to death as CV events.

In summary, the work presented in this chapter supports that the PWA-drop mean area under the curve is associated with prevalent hypertension suggesting that PWA-drops could be useful clinical marker. Future work to examine PWA features predictive of future events in longitudinal studies, larger other cohorts and with targeted treatments would be useful to help clarify the potential role of frequent cardiovascular activation responses in contributing to cardiovascular disease.

CHAPTER 5 – PULSE WAVE AMPLITUDE DROPS IN RESPONSE TO ENVIRONMENTAL NOISE DURING SLEEP

5.1 Introduction

Noise can provoke autonomic and cortical nervous system responses and thus PWA-drops, HR changes and EEG arousals could be sensitive sleep disturbance markers of environmental noise disturbance. The aim of this chapter was to explore these sleep disturbance markers in a small pilot study (N = 24) in which participants were exposed to a range of environmental noises at various sound pressure levels. The noise samples included wind farm noise as this has recently been associated with sleep problems and complaints, yet the evidence to support this is poor.

5.2 Methodology

5.2.1 Data collection

Participants and experimental conditions

Twenty-four individuals, including 11 males (26.4 ± 16.3 years, age range: 18 - 75 years) and 13 females (24.4 ± 9.3 years, age range: 19 - 55 years) were recruited for a one-night sleep study. Participants were screened to select good sleepers with normal hearing and without significant medical and/or psychiatric conditions. Basic auditory assessments were conducted via an audiometer for assessing hearing acuity. Participants' lights out time was determined by averaging habitual bedtime from a one week's sleep diary kept at home prior to the laboratory study. Wake-up time was not controlled.

Physiological recordings

For the sleep study, participants were instrumented with polysomnography (PSG) equipment including electroencephalogram (EEG; F3, F4, C3, C4, Cz, O1 and O2), electro-oculogram (EOG; E1 and E2), chin electromyogram (EMG), leg movements (leg EMG), electrocardiogram (ECG) and finger pulse oximetry. Simultaneous acoustic and sleep study recordings were time-locked via timing marks recorded simultaneously on both devices.

Auditory tones and controls

For the sleep study, a battery of block-randomised noise stimuli of 20 seconds duration, interspersed with 20-second silent periods were presented only when participants were asleep (at least 5 minutes into sleep at the start of the protocol and after at least 1 minute of stage 2 or deeper sleep on any subsequent return to sleep after an awakening). The 20 s noise battery during sleep included noise levels ranging from 33 to 48 dB(A), in 3 dB(A) increments, of the following noise types:

- traffic noise short range (TFN short-range) recorded 20 m from a main road,
- traffic noise long range (TFN long-range) recorded 700 m from a main road,
- WFN with amplitude modulation (AM) (WFN AM) recorded 3.3 km from a South Australian wind farm,
- WFN without AM (WFN NOAM) recorded 3.3 km from the same wind farm,
- "Swish" – WFN AM recorded 500 m from the same wind farm,
- silence (background noise control).

During wakefulness, participants were exposed to either silence or WFN AM at 33 dB(A) in random order. The lowest sound pressure level was set at 33 dB(A) to ensure a minimal 10 dB(A) difference between the background noise (23 dB(A)) and noise stimuli. Each noise stimuli was ceased if the participant woke during the night (any EEG return to wake lasting 15 seconds or more) until the participant fell back to sleep, at which point the noise battery was re-started. An independent qualified sleep technician, blinded to the study aims and conditions, scored the sleep data according to American Academy of Sleep Medicine (AASM) criteria.

5.2.2 Cardiovascular markers

The R-wave peaks in the ECG signal were detected with the Hamilton-Tompkins algorithm (Hamilton and Tompkins, 1986) from where the instantaneous beats-per-minute (BPM) were evaluated. Given that the instantaneous beat-to-beat measures of HR and PWA occur at unevenly spaced R-R intervals, a cubic spline interpolation was used to align the responses relative to the noise onset to allow for ensemble averaging.

To help account for substantial variability in signals from heart beat-to-beat and over time, HR and PWA signals were normalised by expressing values as a percentage of the preceding 5 or 10 seconds prior to stimuli onset baseline for HR and PWA, respectively. Note that 20 seconds out of 30 seconds represents the stimuli length.

5.2.3 Statistical analysis

The hazard ratios for sound pressure level and noise type groups, as compared with silent controls, and the corresponding confidence intervals were estimated with the use of a stratified Cox proportional-hazard model. Survival curves for each group were estimated with the use of the Kaplan–Meier method and pairwise comparison was performed using the log-rank test. Rates at fixed time points were derived from the Kaplan–Meier estimate, along with their corresponding 95% confidence interval. Null hypotheses were rejected when $p < 0.05$.

The survival curves using the Kaplan-Meier method were estimated for the following groups:

- 7 groups of sound pressure level: Silence/Control, 33 dB(A), 36 dB(A), 39 dB(A), 42 dB(A), 45 dB(A) and 48 dB(A),
- 6 groups of noise type: Silence/Control, TFN short-range, TFN long-range, WFN AM, WFN NOAM and “Swish”,
- 3 groups of sleep: Stage 2, Stage 3 (deep sleep) and REM sleep.

Survival curves show the probability of a response, PWA-drop or EEG arousal, occurring up until a specific point in time. When a survival curve decreases more abruptly than another, it means that participants experienced more PWA responses due to noise in this condition than the other condition. Numbers at risk were also determined to show the absolute number of participants still event-free and still at risk each 5 seconds out of the total 40 second period of analysis. The Cox proportional hazards regression model allows testing for differences in survival times of multiple groupings of predictor variables. Cox regression models were performed at 5 second cut-off time values. The sound pressure levels (SPLs) of the noise, the noise types and the sleep stages in which the noise occurred used in the Kaplan-Meier method were studied as potential predictors of evoked PWA responses. The hazard ratio of each variable relative to the relevant reference category is an indicator of predictive utility, where a hazard ratio significantly below 1 or above 1 indicates a predictor of reduced or increased incidence of the selected outcome event, respectively. Statistical analysis was performed using packages Survival version 2.44-1.1 and Survminer version 0.4.6 in R.

5.3 Results

5.3.1 Characteristic PWA and HR responses

This section presents results of the two cardiovascular marker responses occurring during Stage 2, Stage 3 and REM sleep grouped into “quiet” and “loud” conditions for one participant as an example. Table 6 shows the number of delivered noise samples which triggered a PWA-drop within the first 5 seconds after noise onset. The 5 second cut-off value was chosen because it was previously shown that PWA-drops occur within that time frame (Griefahn, 2017, Catcheside et al., 2002). PWA-drops occurred in response to 17% of the noise stimuli with no statistically significant difference in propensity between “quiet” and “loud” groups (Fisher’s test, $p = 0.404$).

Table 6: Summary of the PWA-drops in “quiet” and “loud” groups occurring in Stage 2, Stage 3 and REM sleep for one participant.

	Total N	Present	Absent
“Quiet” (33-39 dB(A))	246	38 (15.4%)	208 (84.6%)
“Loud” (42-48 dB(A))	250	46 (18.4%)	204 (81.6%)
Total	496	84 (16.9%)	412 (83.1%)

In the “quiet” and “loud” conditions, the average PWA responses, when present 5 seconds after noise onset, were similar with a decrease of approximately 50% amplitude compared to the baseline, as shown in Figure 19. All PWA-drops in this figure were centred with their beginning at time 0 (see Figure 19A and Figure 19C). They were then assemble averaged, and the resulting signals are shown in Figure 19B and Figure 19D. The HR response showed a brief transient acceleration of around 6% up to approximately 5 seconds after noise onset, then returned to baseline around 10 seconds after noise onset.

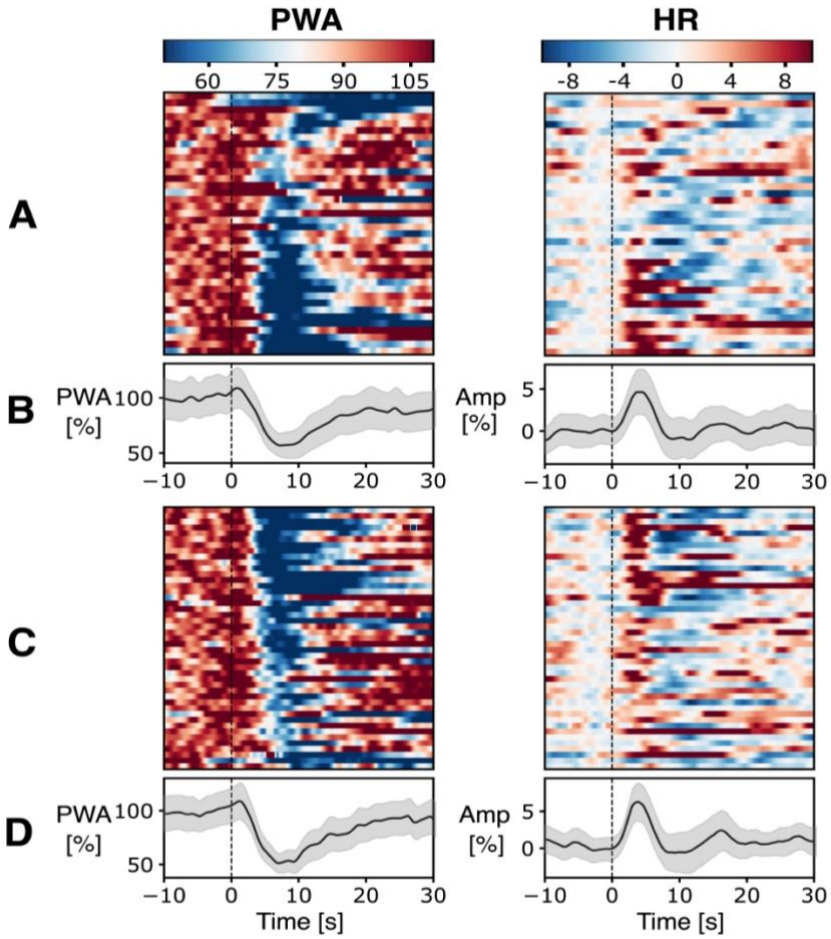

Figure 19: Typical PWA and HR in response to “quiet” (A and B) and “loud” (C and D) noise stimuli together with a spectrogram showing all responses during Stage 2, Stage 3 and REM sleep when a PWA-drop was present 5 seconds after noise onset. Time 0 indicates onset of a 20-second long noise stimuli.

In the case where a PWA response was not present 5 seconds after noise onset, the two cardiovascular markers both fluctuated around the baseline with minimal indication of systematic changes temporally related to the noise onset.

5.3.2 Survival probability of PWA-drops for SPLs

Table 7 summarises the results from a pairwise comparison of PWA-drop occurrence for the SPL factor at 5 seconds after noise onset. The SPL factor seems to impact PWA responses during the 5 first seconds after noise onset, however only SPLs equal or higher than 39dBA were significantly different from the control.

Table 7: P-values of a pairwise comparison between noise levels at 5 seconds after noise onset.

	Control	33dBA	36dBA	39dBA	42dBA	45dBA
33dBA	0.4015	-	-	-	-	-
36dBA	0.1812	0.5590	-	-	-	-
39dBA	0.0050	0.0665	0.1924	-	-	-
42dBA	3.9e-05	0.0024	0.0126	0.2289	-	-
45dBA	5.2e-13	2.1e-09	5.0e-08	3.8e-05	0.0039	-
48dBA	< 2e-16	4.4e-13	1.6e-11	5.0e-08	2.5e-05	0.1924

A Cox regression model performed with SPL showed that SPLs above 39 dB(A) showed statistically significantly higher hazard ratios compared to silence ($p < 0.05$) as shown in Figure 20. The figure also shows an increasing hazard ratio with increasing SPL. At 33 dB(A), the hazard ratio was not statistically significantly different compared to control ($p = 0.39$), but at 39 dB(A) and 48 dB(A), the hazard ratios were 50% and 190% compared to control, respectively ($p = 0.003$ and $p < 0.001$). This means that a PWA-drop had 50% and 190% more chance of occurring during the first 5 seconds after a noise onset at 39 dB(A) and 48 dB(A), respectively, compared to silence. In comparison, a Cox regression model was also performed with EEG arousals (Figure 21), where only SPLs at 42 dB(A) and 48 dB(A) SPLs were associated with a significantly higher probability of provoking a EEG arousal within first 5 seconds of noise onset ($p < 0.05$).

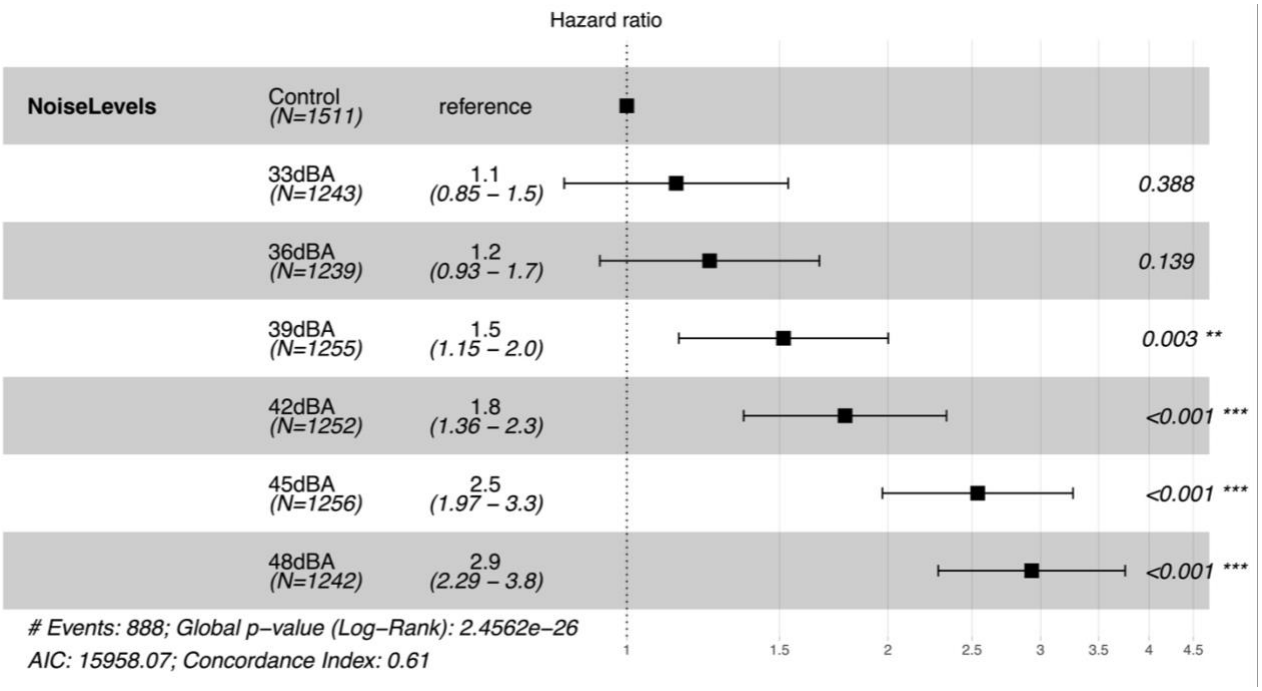

Figure 20: Comparison between PWA-drop hazard ratios for environmental noise at several sound pressure levels. Squares represent point estimates; bars represent 95% confidence limits. Ratios more than 1 indicate that PWA-drops occur more often with noise than when no noise is played during sleep.

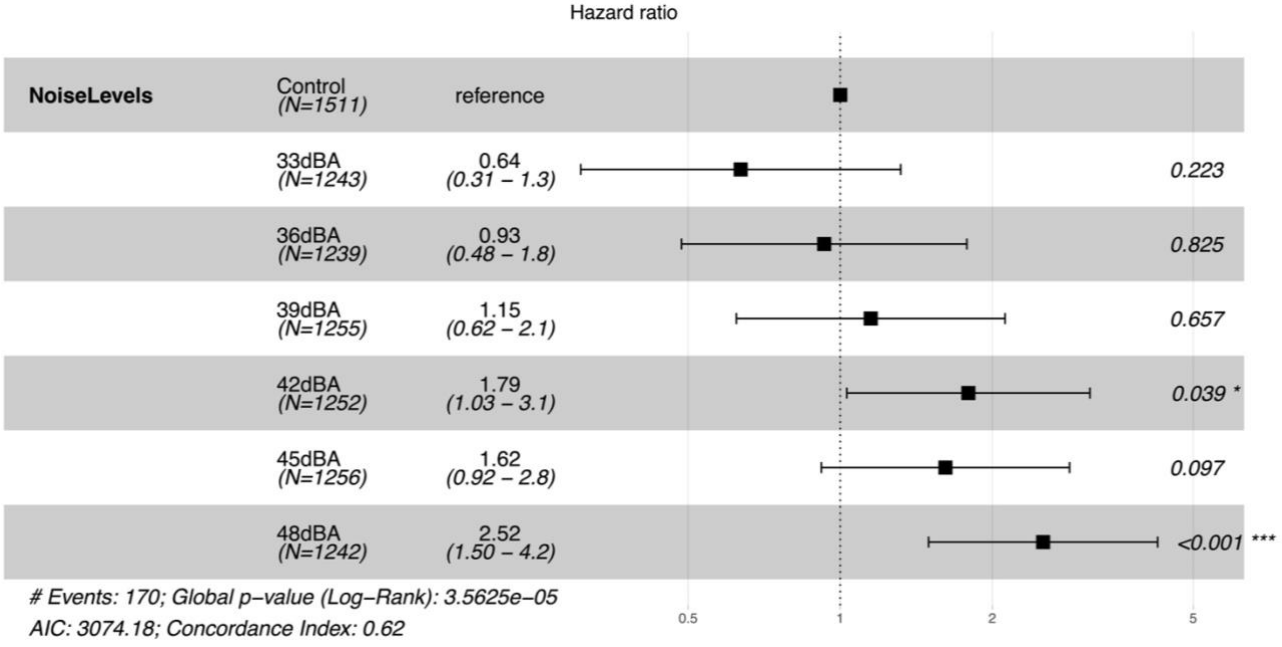

Figure 21: Comparison between EEG arousal hazard ratios for environmental noise at several sound pressure levels during sleep. Squares represent point estimates; bars represent 95% confidence limits. Ratios more than 1 indicate that EEG arousals occur more often with noise than when no noise is played.

Another Cox regression model was performed adjusted for grouped noise SPLs, also with a cut-off value of 5 seconds. The SPL groups were as follows:

- control with “silence”,
- “quiet” with SPLs between 33 dB(A) and 39 dB(A),
- “loud” with SPLs between 42 dB(A) and 48 dB(A).

In both groups the PWA-drop occurrence was significantly higher compared to the control (hazard ratio = 1.3, $p = 0.03$ for “quiet” and hazard ratio = 2.4, $p < 0.001$ for “loud”). The corresponding Kaplan-Meier curves are shown in Figure 22, demonstrating that PWA-drop responses occurred 14%, 8% and 6% of the time for “loud”, “quiet” and control conditions, respectively. After 5 seconds, the survival differences between groups clearly reduce and diminish by around 20 seconds, which is the time when the noise samples stopped playing. At that time, the PWA-drop responses occurred for 24%, 23% and 24% for “loud”, “quiet” and control groups.

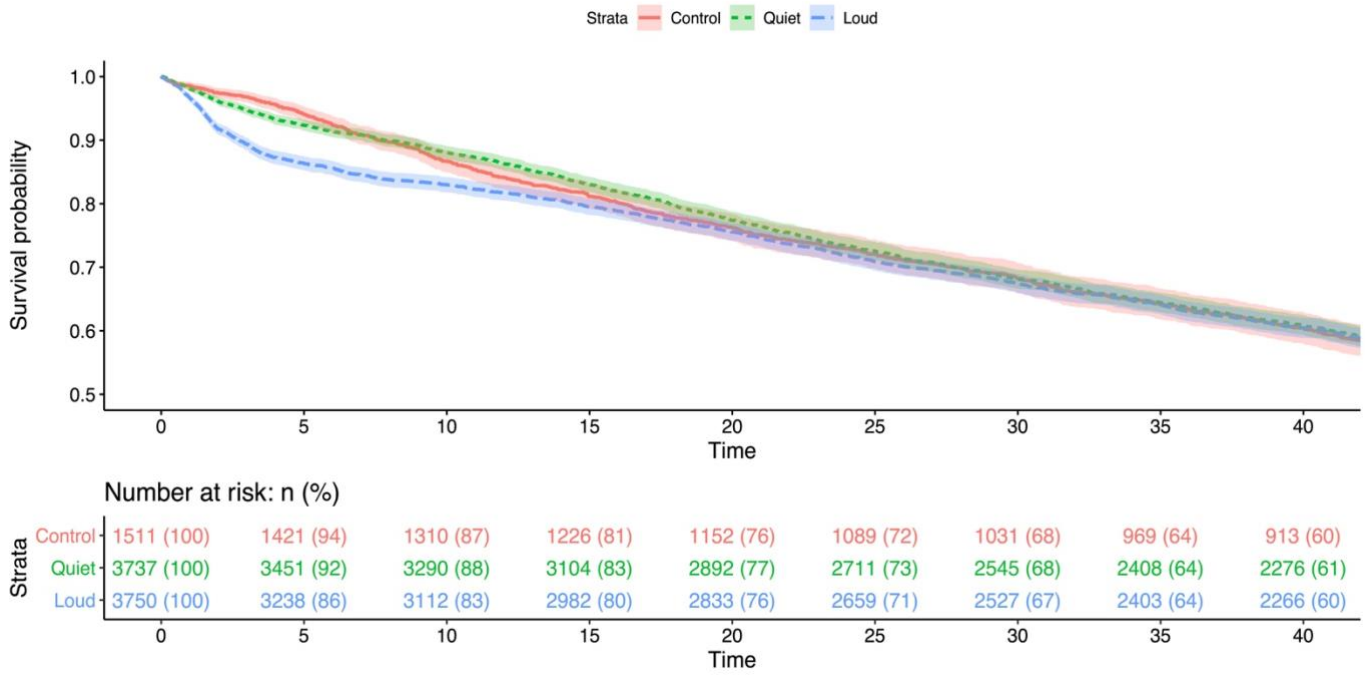

Figure 22: Kaplan-Meier survival curves for PWA-drop occurrence after noise onset adjusted for 3 sound pressure level groups; silence (control), “quiet” and “loud”. Each noise stimulus lasted 20 s after which there was 20 s of silence prior to the next noise stimulus.

The survival functions for noise levels appear to converge after 20 seconds suggesting that noise-evoked and spontaneous responses may not be additive. This could potentially indicate that noise-evoked responses reduce subsequent spontaneous response probability, or that noise-evoked response probability is relatively low and thus potentially difficult to distinguish from that of more common spontaneous responses over time.

5.3.3 Survival probability of PWA-drops for noise type

Another Cox regression model was performed on the noise types with their associated level groups (“quiet” or “loud”), as shown in Figure 23. These results suggest that wind farm noise with and without amplitude modulation only affected PWA responses in the “loud” condition. “Swish” noise, TFN short-range and TFN long-range affected the responses for all group level conditions.

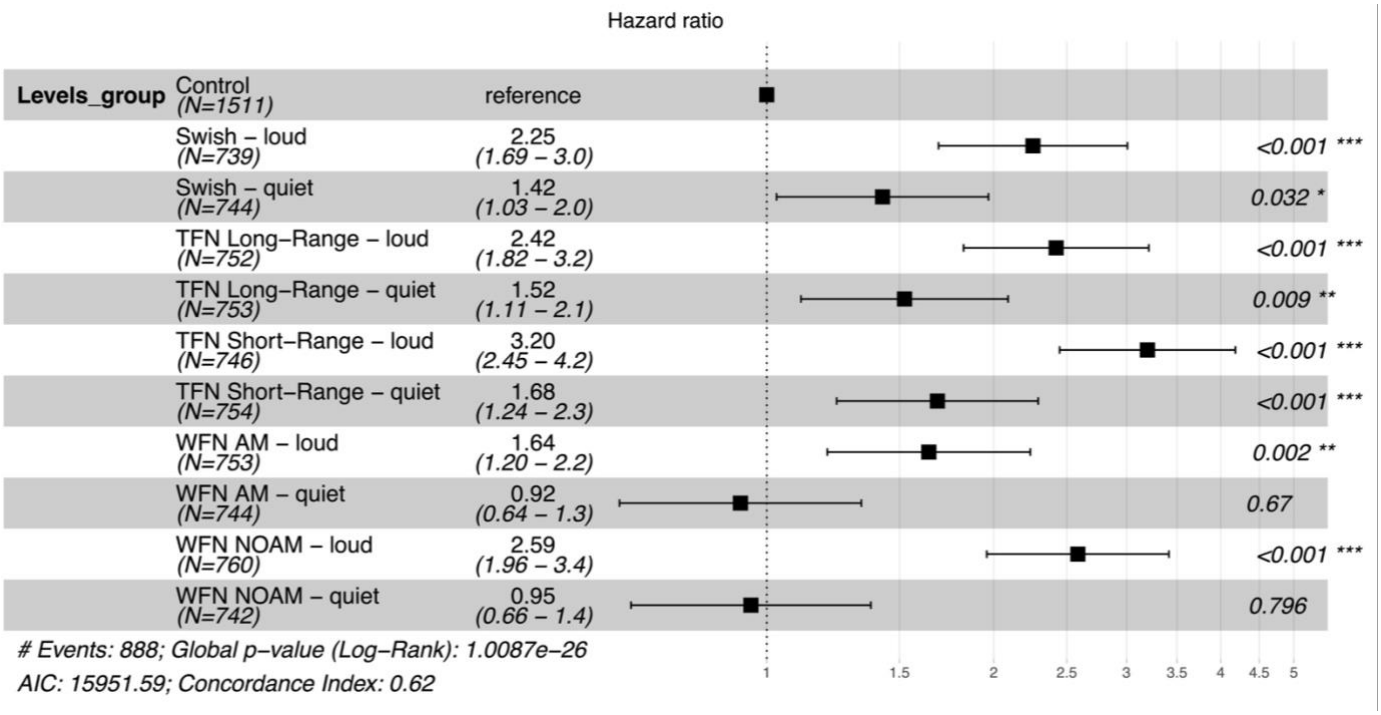

Figure 23: Comparison between PWA-drop hazard ratios for different noise types with their associated level group. Squares represent point estimates; bars represent 95% confidence limits. Ratios more than 1 indicate that PWA-drops occur more often with noise than when no noise is played during sleep.

Kaplan-Meier plots (Figure 24) revealed that all noise types are associated with an increased probability of PWA-drops after noise onset relative to control. PWA responses occurred 205 times (14%) of all traffic noise short-range presentations at 5 seconds after noise onset and was the noise type with the most PWA responses. On the other hand, wind farm noise with amplitude modulation was the type of noise with the least PWA responses at 5 seconds after noise onset; 113 times (8%). Moreover, as seen with the pairwise comparison between noise types (

Table 8), all noise types showed statistically significant differences compare to control except for the wind farm noise with amplitude modulation.

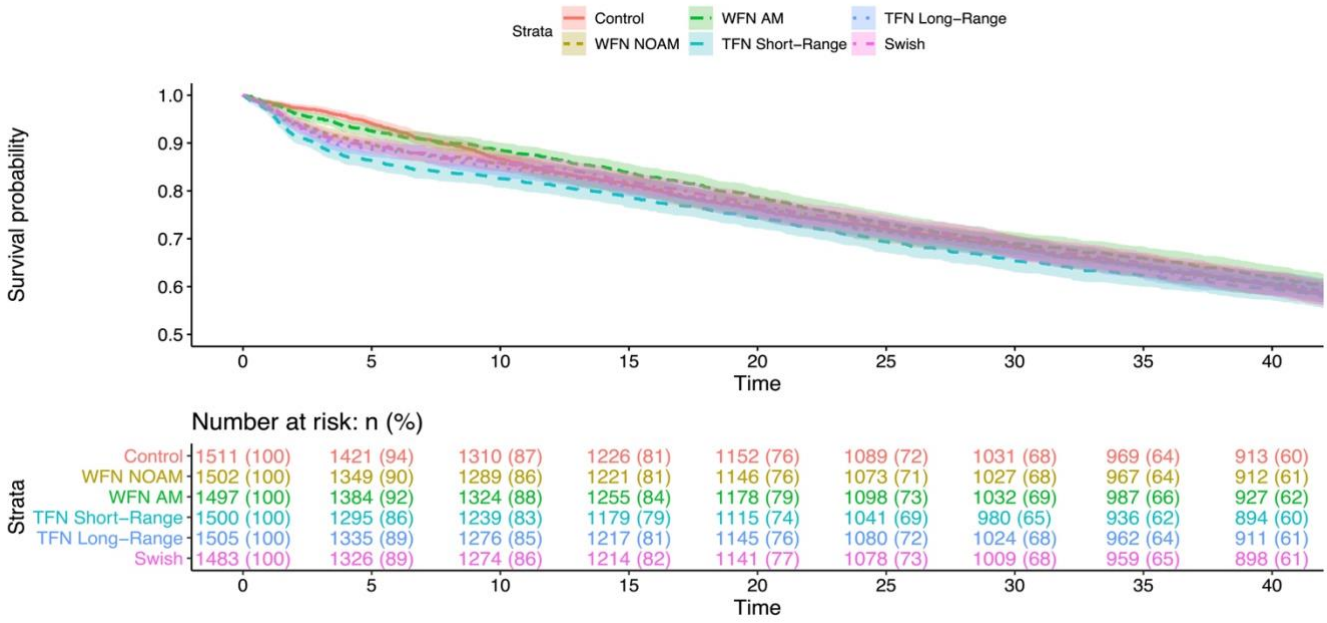

Figure 24: Kaplan-Meier survival curve showing PWA-drop occurrence after noise onset (20 s stimuli followed by 20 s of silence) adjusted for 7 noise types; silence, WFN NOAM, WFN AM, TFN short-range, TFN long-range and “Swish”.

Table 8: P-values of a pairwise comparison between noise types at 5 seconds after noise onset.

	Control	Swish	TFN Long-Range	TFN Short-Range	WFN AM
Swish	1.2e-05	-	-	-	-
TFN Long-Range	6.3e-07	0.5699	-	-	-
TFN Short-Range	9.3e-12	0.0149	0.0637	-	-
WFN AM	0.0990	0.0063	0.0009	2.7e-07	-
WFN NOAM	4.9e-05	0.7166	0.3710	0.0063	0.0149

5.3.4 Survival probability of PWA-drops controlled for sleep stage

Multiple Cox regression models were examined to test the effects of noise type and level (“quiet” or “loud”) for three sleep stages (Stage 2, Stage 3 and REM sleep). Both Stage 2 and Stage 3 showed overall statistically significant effects of noise types and associated levels ($p < 0.001$). Within sleep Stage 2, all noise types showed a higher hazard ratio than the reference case of silence (control), except for wind farm noise with and without amplitude modulation for the “quiet” condition (Figure 25). Moreover, for sleep Stage 3, only the “loud” condition showed a higher hazard ratio than the reference silence in the same sleep stage (Figure 26). However, during REM sleep, there were no statistically significant differences compare to the silence reference for any “loud” or “quiet” noise type (Figure 27).

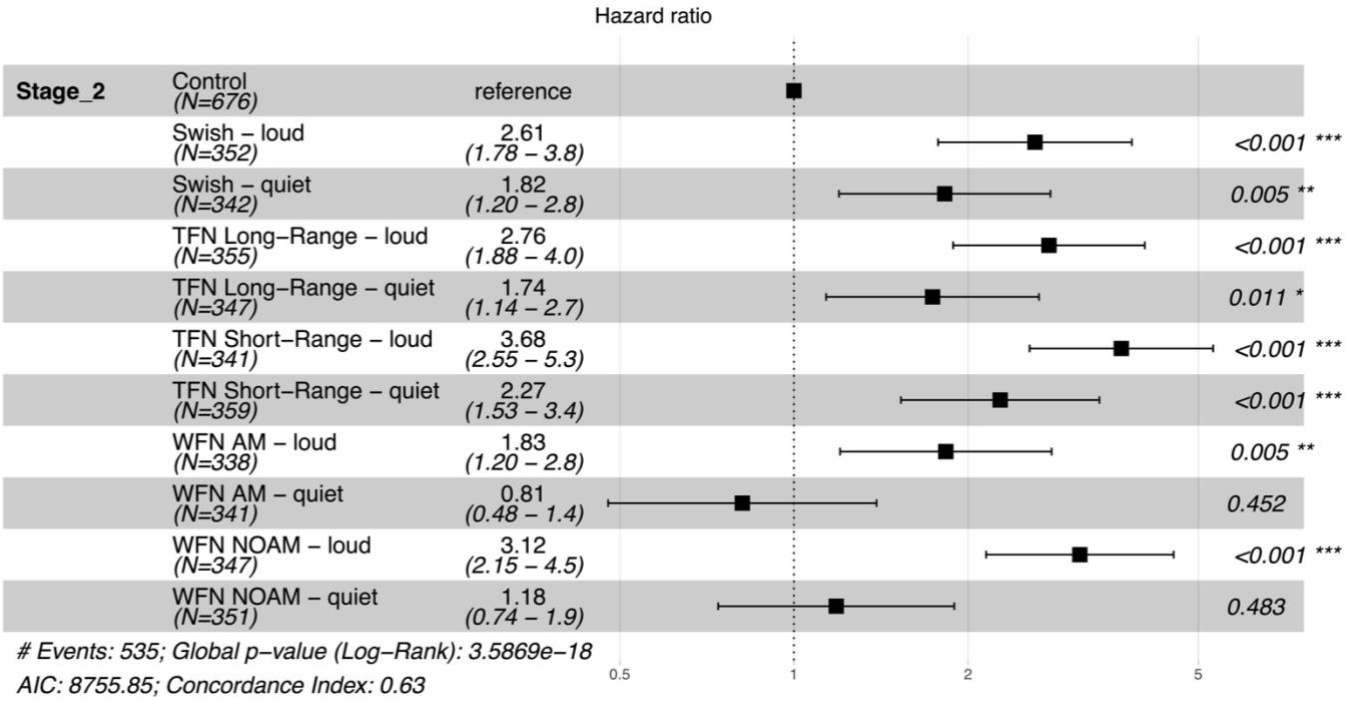

Figure 25: Comparison between PWA-drop hazard ratios for different noise types with their associated level group during sleep Stage 2. Squares represent point estimates; bars represent 95% confidence limits. Ratios more than 1 indicate that PWA-drops occur more often with noise than when no noise is played during sleep.

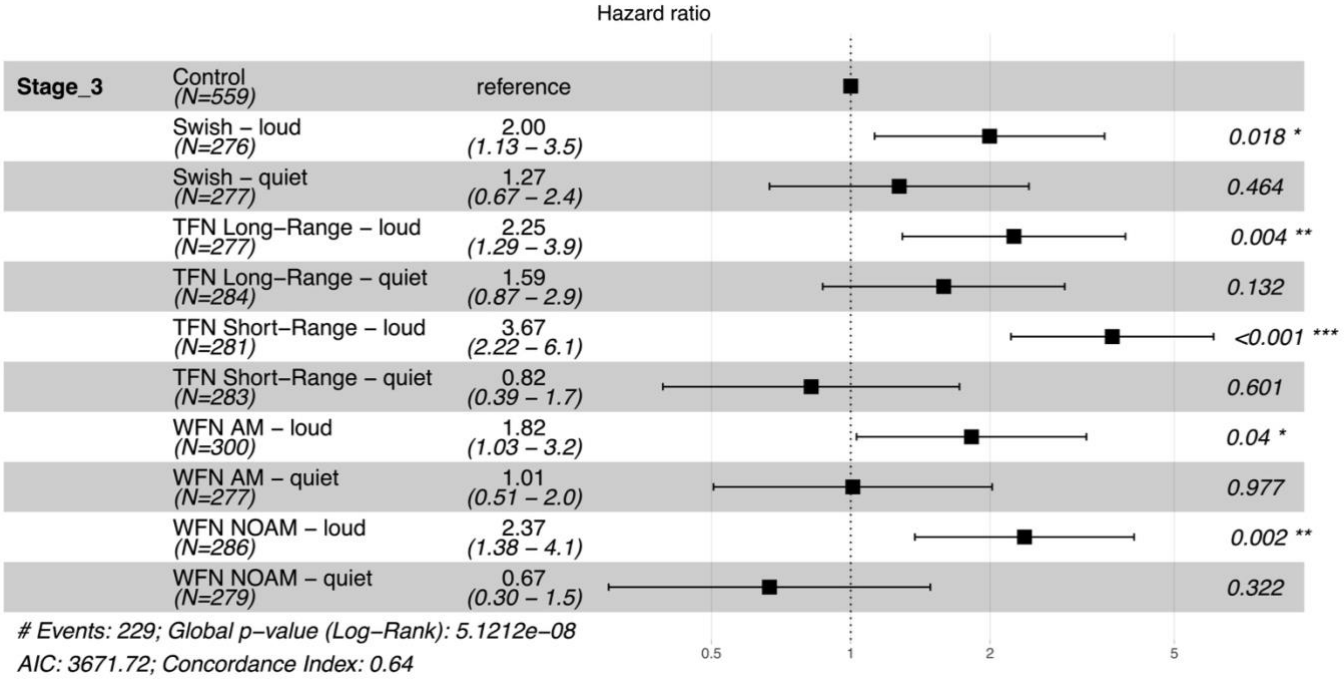

Figure 26: Comparison between PWA-drop hazard ratios for different noise types with their associated level group during sleep Stage 3. Squares represent point estimates; bars represent 95% confidence limits. Ratios more than 1 indicate that PWA-drops occur more often with noise than when no noise is played during sleep.

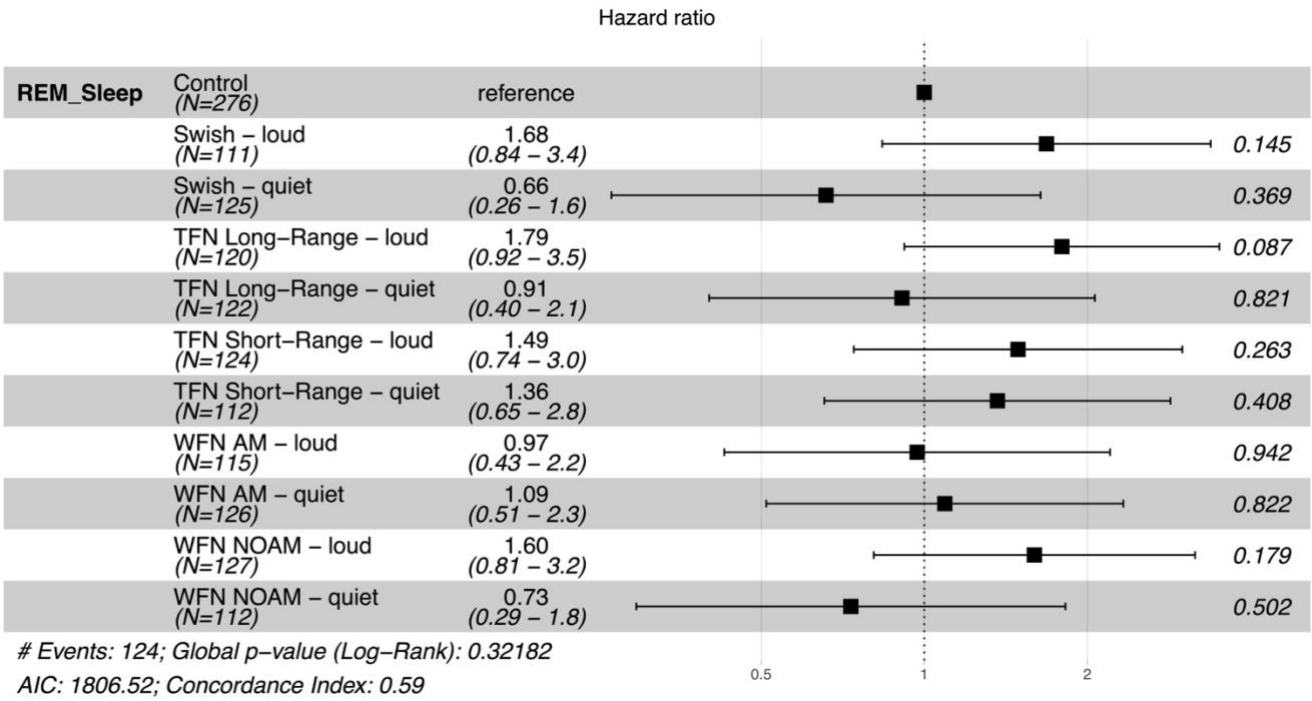

Figure 27: Comparison between PWA-drop hazard ratios for different noise types with their associated level group during REM sleep. Squares represent point estimates; bars represent 95% confidence limits. Ratios more than 1 indicate that PWA-drops occur more often with noise than when no noise is played during sleep.

The Kaplan-Meier curves of sleep stage effects support that PWA responses occurred the least frequently during sleep Stage 3 (Figure 28). Sleep Stage 2 seems to be the sleep stage with the highest propensity for PWA responses during the first 5 seconds after noise onset, followed by REM sleep and finally sleep Stage 3. The survival functions for sleep Stage 3 do not merge after 20 seconds unlike those for Stage 2 and REM sleep suggesting that PWA occurrence is strongly dependent on sleep stage, with less frequent PWA responses in Stage 3 compared to Stage 2 and REM sleep.

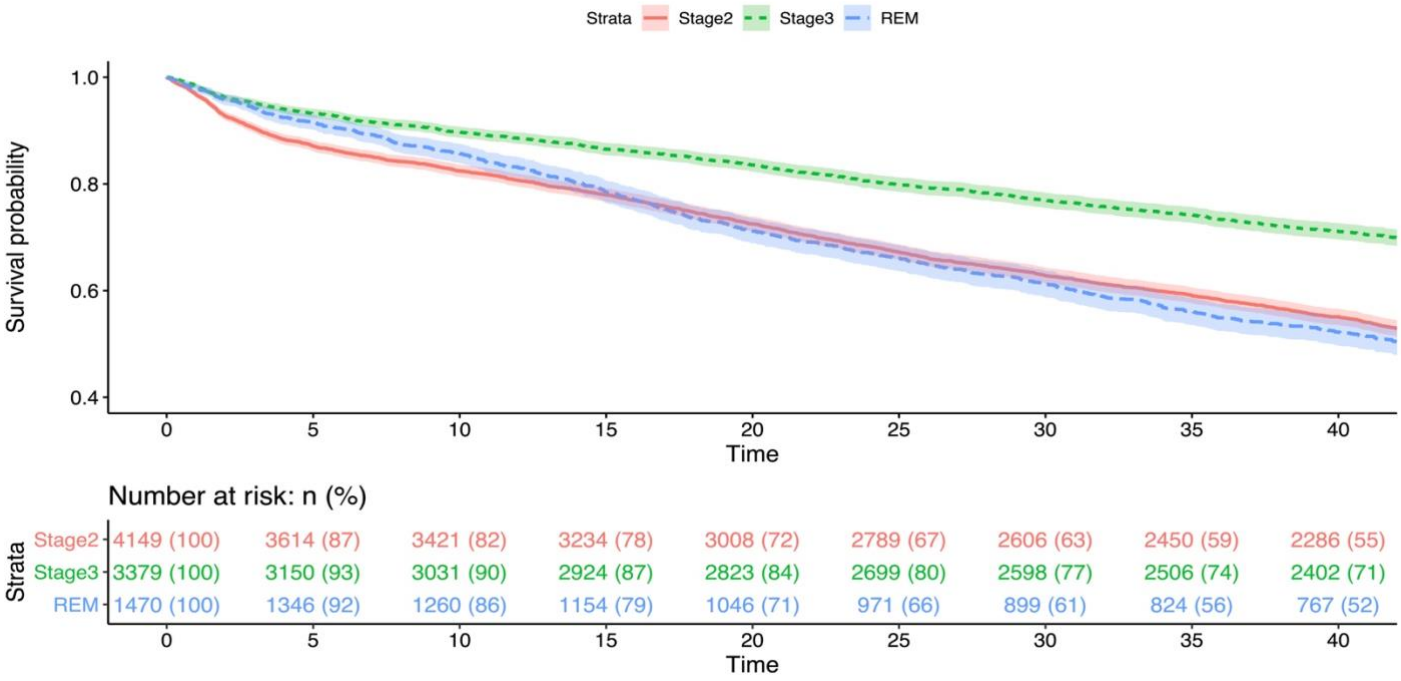

Figure 28: Kaplan-Meier survival curve showing PWA-drop occurrence after noise onset (20 s stimuli followed by 20 s of silence) adjusted for 3 sleep stages; Stage 2, Stage 3 and REM sleep.

The pairwise comparison between sleep stage at 5 seconds after noise onset showed that Stage 2 seems to be the sleep stage when noise has the highest impact on PWA responses during the 5 first seconds after noise onset (Stage 2 vs Stage 3: $p < 2e\text{-}16$ and Stage 2 vs REM sleep: $p = 7.5e\text{-}06$). However, pairwise comparisons between sleep stages at 20 seconds after noise onset showed that Stage 3 had the lowest propensity for PWA response (Stage 3 vs Stage 2: $p < 2e\text{-}16$ and Stage 3 vs REM sleep: $p < 2e\text{-}16$).

5.4 Discussion

The principal finding of this study was that environmental noise with an SPL of 39 dB(A) SPL or higher evokes more PWA-drops than occur without noise presentations during sleep. The PWA-drops generally seem to occur in the first 5 seconds after noise onset.

The amplitude of the average PWA response decreased for a period greater than 30 seconds, and the average HR response accelerated to its maximum around 5 seconds and then decelerated back to baseline within around 10 seconds, consistent with previous findings (Griefahn, 2017, Tassi et al., 2010, Catcheside et al., 2002). These results likely reflect sympathetic nervous system activation which largely controls PWA and HR responses (Di Nisi et al., 1990). Moreover, the magnitude of signal decrease (approximately 50%) for the PWA response was similar to previous findings (Catcheside et al., 2002) despite substantially lower SPLs and stimuli type used in this study 33 to 48 dB(A) versus 54 to 90 dB (Catcheside et al., 2002). Furthermore, no strong differences between “quiet” and “loud” noise groups are also

consistent with an “all or none” PWA response phenomenon.

The strong relationship between SPL and PWA response is perhaps not surprising given previous findings (Griefahn, 2017) and is consistent with an increased likelihood of response with increasing SPLs shown by Catcheside et al. (2002) and Tassi et al. (2010). Moreover, the PWA response seems to be more sensitive at lower SPLs than evoked EEG arousals.

In this study, short-range traffic noise was found to have the highest impact on the PWA response. This noise type has a spectrum dominated by mid-frequency energy. On the other hand, wind farm noise with low-frequency amplitude modulation showed the least impact on the PWA response.

During deeper sleep (Stage 3), fewer PWA responses were present compared to Stage 2 sleep which was in accordance with previous findings (Griefahn, 2017, Muzet, 2007) suggesting a lower cardiovascular response threshold during deep sleep. Moreover, in REM sleep, results by noise types separated in groups of “quiet” and “loud” conditions were not statistically significant, which may be due to a smaller number of events during this stage. However, PWA responses were more likely to occur 5 seconds after noise onset during sleep Stage 2.

In summary, this study supports that PWA-drops are a more sensitive marker of noise disturbances during sleep compared to heart rate changes and EEG responses. SPL seems to be the most influential factor on PWA responses. Nonetheless, the noise type and sleep stage also seem to have an impact on the PWA response. Future work to examine a larger population exposed to more different noise types would be useful to help establish which component of the noise (amplitude modulation, low frequency, etc.) is the most influential on the cardiovascular system during sleep.

CHAPTER 6 – CONCLUSION AND FUTURE WORK

Two algorithms were developed and assessed against consensus scoring of two expert human scorers. The moving window algorithm was chosen for this study due to a slightly higher F1-score in the consensus dataset. This algorithm could overcome issues of intra-scorer variability, increase the efficiency of detecting PWA-drops, operate independently of conventional sleep stage scoring and demonstrate more consistent detection than human scorers. However, the absence of general guidelines poses issues about the definition of a PWA-drops as a threshold of 30% amplitude decrease is inevitably somewhat arbitrary. A lower amplitude decrease threshold would potentially be less conservative and allow the assessment performance of algorithm detection for even more subtle PWA response changes. However, a threshold set too low relative to beat-to-beat pulse wave amplitude and device measurement variability would likely detect substantially more events that may or may not be clinically informative regarding real underlying autonomic responses during sleep. Whilst beyond the scope of the work presented in this thesis, ultimately, a more systematic evaluation to explore relationships between response detection thresholds and clinical endpoints such as incident hypertension and cardiovascular events is likely to be needed to further refine these methods.

Whether or not PWA-drops could be a marker of cardiovascular risk was investigated via the analysis of two large cohort datasets; MAILES and HypnoLaus. The use of the HypnoLaus cohort was designed to help cross-validate the results of association between PWA-drop features and prevalent hypertension and cardiovascular disease found previously (Hirotsu et al., 2020). The PWA-drop mean area under the curve was associated with hypertension and was found to be the most consistent PWA-drop feature across the MAILES and HypnoLaus study datasets. However, no consistent findings were observed between PWA-drop features and prevalent cardiovascular disease across datasets. Differences between populations such as body mass index, apnoea-hypopnoea index as well as gender in the two cohorts might help to explain why no consistent findings were found between datasets except for PWA-drop mean area under the curve. The MAILES study was a cohort of only men from Australia and HypnoLaus was a Lausanne Switzerland population-based cohort. The relatively small number of previous cardiovascular events limiting study power might also help to explain these findings. Therefore, a more uniform and bigger dataset might be needed to more definitively establish if associations exist between PWA-drop features and prevalent cardiovascular disease. Nevertheless, the PWA-drop mean area under the curve was consistently associated with prevalent hypertension and suggests that PWA-drops could be a useful clinical marker of cardiovascular disturbance during sleep and future adverse outcome risks. These findings clearly warrant further studies in larger and longitudinal cohort studies.

The dose-response relationship between environmental noise evoked PWA-drops was investigated to examine PWA-drops as a marker of noise-induced sleep disturbance. Noise characteristics, such as sound pressure levels and type, as well as sleep staging were investigated as potential mediators in the dose-response between PWA-drop and noise. It was found that in comparison to heart rate and EEG arousal responses, PWA-drops occurred more often at lower sound pressure levels and, showed longer duration and larger amplitude responses compared to heart rate changes and EEG responses, supporting that PWA-drops are a more sensitive marker of noise disturbances during sleep. Noise sound pressure levels appeared to be the most influential factor on PWA-drops compared to noise types or the sleep stage in which noise occurred. The main limitation of this part of the study was that the sample size may not have been sufficient to reliably determine which noise types and which specific sound pressure levels had the largest effect on PWA-drops. Thus, it was not possible to definitively establish if wind farm noise, with or without amplitude modulation, had a differential effect on PWA-drops compared to traffic noise. Thus, further studies are needed to help establish if the amplitude modulation component of wind farm noise has a significant impact on the cardiovascular system during sleep.

In conclusion, finger photoplethysmography is a simple, non-invasive, affordable and already widely available method from which PWA-drops can be derived. The algorithm developed and validated in the first chapter was used to determine the potential utility of PWA-drops as a marker of sleep disturbance in response to noise as well as a marker of the cardiovascular system during sleep associated with cardiovascular pathophysiology. PWA-drops during sleep appear to be a reliable marker of cardiovascular system disturbances during sleep.

Although the results of this project support that PWA-drops are a reliable marker of cardiovascular disturbances during sleep, more work is required to further examine if PWA-drop features are associated with prevalent and incident hypertension and future cardiovascular events. Moreover, future studies should also examine relationships between noise exposure and cardiovascular outcomes to explore the potential of noise-induced PWA-drops as a marker of increased cardiovascular risk. Furthermore, a larger population exposed to different noise types should be studied to try to determine if noise characteristics (low-frequency, high-frequency, amplitude modulation, etc.) influence PWA responses and cardiovascular outcome risks.

REFERENCES

AHN, R., BURKE, T. F. & MCGAHAN, A. M. 2015. *Innovating for Healthy Urbanization*.

APPLETON, S. L., VAKULIN, A., MARTIN, S. A., LANG, C. J., WITTERT, G. A., TAYLOR, A. W., MCEVOY, R. D., ANTIC, N. A., CATCHESIDE, P. G. & ADAMS, R. J. 2016. Hypertension Is Associated With Undiagnosed OSA During Rapid Eye Movement Sleep. *Chest,* 150**,** 495-505.

BABISCH, W. 2011. Cardiovascular effects of noise. *Noise Health,* 13**,** 201-4.

BACH, V., LIBERT, J. P., TASSI, P., WITTERSHEIM, G., JOHNSON, L. C. & EHRHART, J. 1991. Cardiovascular responses and electroencephalogram disturbances to intermittent noises: effects of nocturnal heat and daytime exposure. *Eur J Appl Physiol Occup Physiol,* 63**,** 330-7.

BASNER, M., BABISCH, W., DAVIS, A., BRINK, M., CLARK, C., JANSSEN, S. & STANSFELD, S. 2014. Auditory and non-auditory effects of noise on health. *The Lancet,* 383**,** 1325-1332.

BASNER, M. & MCGUIRE, S. 2018. WHO Environmental Noise Guidelines for the European Region: A Systematic Review on Environmental Noise and Effects on Sleep. *Int J Environ Res Public Health,* 15.

BASNER, M., MULLNER, U. & GRIEFAHN, B. 2010. Practical guidance for risk assessment of traffic noise effects on sleep. *Applied Acoustics,* 71**,** 518-522.

BAUST, W. & BOHNERT, B. 1969. The regulation of heart rate during sleep. *Experimental Brain Research,* 7**,** 169-180.

BERGLUND, B., LINDVALL, T. & SCHWELA, D. H. 1999. Guidelines for community noise.

BERRY, R. B., BUDHIRAJA, R., GOTTLIEB, D. J., GOZAL, D., IBER, C., KAPUR, V. K., MARCUS, C. L., MEHRA, R., PARTHASARATHY, S., QUAN, S. F., REDLINE, S., STROHL, K. P., DAVIDSON WARD, S. L., TANGREDI, M. M. & AMERICAN ACADEMY OF SLEEP, M. 2012. Rules for scoring respiratory events in sleep: update of the 2007 AASM Manual for the Scoring of Sleep and Associated Events. Deliberations of the Sleep Apnea Definitions Task Force of the American Academy of Sleep Medicine. *Journal of clinical sleep medicine : JCSM : official publication of the American Academy of Sleep Medicine,* 8**,** 597-619.

BERTISCH, S. M., POLLOCK, B. D., MITTLEMAN, M. A., BUYSSE, D. J., BAZZANO, L. A., GOTTLIEB, D. J. & REDLINE, S. 2018. Insomnia with objective short sleep duration and risk of incident cardiovascular disease and all-cause mortality: Sleep Heart Health Study. *Sleep,* 41.

BETTA, M., HANDJARAS, G., RICCIARDI, E., PIETRINI, P., HABA-RUBIO, J., SICLARI, F., HEINZER, R. & BERNARDI, G. 2020. Quantifying peripheral sympathetic activations during sleep by means of an automatic method for pulse wave amplitude drop detection. *Sleep Med,* 69**,** 220-232.

BINGHE, W. & JINGLIN, X. 1998. Detecting system and power-spectral analysis of pulse signals of human body. *Proceedings of the Fourth International Conference on Signal Processing***,** 1646-1649.

BRANDENBERGER, G., EHRHART, J., PIQUARD, F. & SIMON, C. 2001. Inverse coupling between ultradian oscillations in delta wave activity and heart rate variability during sleep. *Clinical neurophysiology : official journal of the International Federation of Clinical Neurophysiology,* 112**,** 992-996.

CATCHESIDE, P. G., CHIONG, S. C., MERCER, J., SAUNDERS, N. A. & MCEVOY, R. D. 2002. Noninvasive cardiovascular markers of acoustically induced arousal from non-rapid-eye-movement sleep. *Sleep,* 25**,** 797-804.

CHEN, H.-C., SU, T.-P. & CHOU, P. 2013. A nine-year follow-up study of sleep patterns and mortality in community-dwelling older adults in Taiwan. *Sleep,* 36**,** 1187-1198.

DI NISI, J., MUZET, A., EHRHART, J. & LIBERT, J. P. 1990. Comparison of cardiovascular responses to noise during waking and sleeping in humans. *Sleep,* 13**,** 108-20.

EBERHARDT, J. L. & AKSELSSON, K. R. 1987. The Disturbance by Road Traffic Noise of the Sleep of Young Male-Adults as Recorded in the Home. *Journal of Sound and Vibration,* 114**,** 417-434.

GRANT, J. F., MARTIN, S. A., TAYLOR, A. W., WILSON, D. H., ARAUJO, A., ADAMS, R. J., JENKINS, A., MILNE, R. W., HUGO, G. J., ATLANTIS, E. & WITTERT, G. A. 2014. Cohort profile: The men androgen inflammation lifestyle environment and stress (MAILES) study. *Int J Epidemiol,* 43**,** 1040-53.

GRIEFAHN, B. Traffic noise effects on autonomic arousals during sleep. 12th ICBEN Congress on Noise as a Public Health Problem, 18-22 June 2017 Zurich.

GRIEFAHN, B., MARKS, A. & ROBENS, S. 2006. Noise emitted from road, rail and air traffic and their effects on sleep. *Journal of Sound and Vibration,* 295**,** 129-140.

GROTE, L., PLOCH, T., HEITMANN, J., KNAACK, L., PENZEL, T. & PETER, J. H. 1999. Sleep-related Breathing Disorder Is an Independent Risk Factor for Systemic Hypertension. *American Journal of Respiratory and Critical Care Medicine,* 160**,** 1875-1882.

GROTE, L., SOMMERMEYER, D., ZOU, D., EDER, D. N. & HEDNER, J. 2011. Oximeter-based autonomic state indicator algorithm for cardiovascular risk assessment. *Chest,* 139**,** 253-259.

GROTE, L. & ZOU, D. 2017. Pulse Wave Analysis During Sleep. *Principles and Practice of Sleep Medicine.*

GROTE, L., ZOU, D., KRAICZI, H. & HEDNER, J. 2003. Finger plethysmography--a method for monitoring finger blood flow during sleep disordered breathing. *Respir Physiol Neurobiol,* 136**,** 141-52.

HAMILTON, P. S. & TOMPKINS, W. J. 1986. Quantitative Investigation of Qrs Detection Rules Using the Mit/Bih Arrhythmia Database. *Ieee Transactions on Biomedical Engineering,* 33**,** 1157-1165.

HEINZER, R., VAT, S., MARQUES-VIDAL, P., MARTI-SOLER, H., ANDRIES, D., TOBBACK, N., MOOSER, V., PREISIG, M., MALHOTRA, A., WAEBER, G., VOLLENWEIDER, P., TAFTI, M. & HABA-RUBIO, J. 2015. Prevalence of sleep-disordered breathing in the general population: the HypnoLaus study. *Lancet Respir Med,* 3**,** 310-8.

HERITIER, H., VIENNEAU, D., FORASTER, M., EZE, I. C., SCHAFFNER, E., THIESSE, L., RUDZIK, F., HABERMACHER, M., KOPFLI, M., PIEREN, R., BRINK, M., CAJOCHEN, C., WUNDERLI, J. M., PROBST-HENSCH, N., ROOSLI, M. & GROUP, S. N. C. S. 2017. Transportation noise exposure and cardiovascular mortality: a nationwide cohort study from Switzerland. *Eur J Epidemiol,* 32**,** 307-315.

HILLMAN, D. R., MURPHY, A. S. & PEZZULLO, L. 2006. The economic cost of sleep disorders. *Sleep,* 29**,** 299-305.

HIROTSU, C., BETTA, M., BERNARDI, G., MARQUES-VIDAL, P., VOLLENWEIDER, P., WAEBER, G., PICHOT, V., ROCHE, F., SICLARI, F., HABA-RUBIO, J. & HEINZER, R. 2020. Pulse wave amplitude drops during sleep: clinical significance and characteristics in a general population sample. *Sleep***,** zsz322.

IBER, C., ANCOLI-ISRAEL, S., CHESSON, A. L. & QUAN, S. 2007. AASM - Manual for the Scoring of Sleep and Associated Events.

JAVAHERI, S., ZHAO, Y. Y., PUNJABI, N. M., QUAN, S. F., GOTTLIEB, D. J. & REDLINE, S. 2018. Slow-Wave Sleep Is Associated With Incident Hypertension: The Sleep Heart Health Study. *Sleep,* 41**,** zsx179.

JOHNSON, L. C. & LUBIN, A. 1967. The orienting reflex during waking and sleeping. *Electroencephalogr Clin Neurophysiol,* 22**,** 11-21.

JORDAN, A. S., ECKERT, D. J., CATCHESIDE, P. G. & MCEVOY, R. D. 2003. Ventilatory response to brief arousal from non-rapid eye movement sleep is greater in men than in women. *Am J Respir Crit Care Med,* 168**,** 1512-9.

KALES, A. & RECHTSCHAFFEN, A. 1968. *A manual of standardized terminology, techniques and scoring system for sleep stages of human subjects. Allan Rechtschaffen and Anthony Kales, editors,* Bethesda, Md, U. S. National Institute of Neurological Diseases and Blindness, Neurological Information Network.

KEEFE, F. B., JOHNSON, L. C. & HUNTER, E. J. 1971. EEG and autonomic response pattern during waking and sleep stages. *Psychophysiology,* 8**,** 198-212.

KENDZERSKA, T., GERSHON, A. S., HAWKER, G., LEUNG, R. S. & TOMLINSON, G. 2014. Obstructive sleep apnea and risk of cardiovascular events and all-cause mortality: a decade-long historical cohort study. *PLoS medicine,* 11**,** e1001599-e1001599.

KRYTER, K. D. & POZA, F. 1980. Effects of noise on some autonomic system activities. *J Acoust Soc Am,* 67**,** 2036-44.
LEE, W. H., AHN, J.-C., WE, J., RHEE, C.-S., LEE, C. H., YUN, P.-Y., YOON, I.-Y. & KIM, J.-W. 2014. Cardiopulmonary coupling analysis: changes before and after treatment with a mandibular advancement device. *Sleep and Breathing,* 18**,** 891-896.
LI, Y., LI, Y., WINKELMAN, J. W., WALTERS, A. S., HAN, J., HU, F. B. & GAO, X. 2018. Prospective study of restless legs syndrome and total and cardiovascular mortality among women. *Neurology,* 90**,** e135-e141.
MCCORRY, L. K. 2007. Physiology of the autonomic nervous system. *American journal of pharmaceutical education,* 71**,** 78-78.
MUNZEL, T., SCHMIDT, F. P., STEVEN, S., HERZOG, J., DAIBER, A. & SORENSEN, M. 2018. Environmental Noise and the Cardiovascular System. *J Am Coll Cardiol,* 71**,** 688-697.
MUZET, A. 2007. Environmental noise, sleep and health. *Sleep Med Rev,* 11**,** 135-42.
MUZET, A. 2011. Sleep Disturbance in Adults by Noise. 83-87.
NEWSON, R. B. 2010. Comparing the predictive powers of survival models using Harrell's C or Somers' D. *Stata Journal,* 10**,** 339-358.
NIETO, F. J., YOUNG, T. B., LIND, B. K., SHAHAR, E., SAMET, J. M., REDLINE, S., D'AGOSTINO, R. B., NEWMAN, A. B., LEBOWITZ, M. D., PICKERING, T. G. & FOR THE SLEEP HEART HEALTH, S. 2000. Association of Sleep-Disordered Breathing, Sleep Apnea, and Hypertension in a Large Community-Based Study. *JAMA,* 283**,** 1829-1836.
ÖHRSTRÖM, E. & SKÅNBERG, A. 2004. Longitudinal surveys on effects of road traffic noise: substudy on sleep assessed by wrist actigraphs and sleep logs. *Journal of Sound and Vibration,* 272**,** 1097-1109.
PILLAR, G., BAR, A., SHLITNER, A., SCHNALL, R., SHEFY, J. & LAVIE, P. 2002. Autonomic arousal index: an automated detection based on peripheral arterial tonometry. *Sleep,* 25**,** 543-9.
PIRRERA, S., DE VALCK, E. & CLUYDTS, R. 2010. Nocturnal road traffic noise: A review on its assessment and consequences on sleep and health. *Environ Int,* 36**,** 492-8.
ROSENTHAL, L. D. & DOLAN, D. C. 2008. The Epworth Sleepiness Scale in the Identification of Obstructive Sleep Apnea. *The Journal of Nervous and Mental Disease,* 196.
SCHNALL, R. P., SHLITNER, A., SHEFFY, J., KEDAR, R. & LAVIE, P. 1999. Periodic, profound peripheral vasoconstriction - A new marker of obstructive sleep apnea. *Sleep,* 22**,** 939-946.
SHAHAR, E., WHITNEY, C. W., REDLINE, S., LEE, E. T., NEWMAN, A. B., JAVIER NIETO, F., O'CONNOR, G. T., BOLAND, L. L., SCHWARTZ, J. E. & SAMET, J. M. 2001. Sleep-disordered Breathing and Cardiovascular Disease. *American Journal of Respiratory and Critical Care Medicine,* 163**,** 19-25.
SILVANI, A. 2008. Physiological Sleep-Dependent Changes in Arterial Blood Pressure: Central Autonomic Commands and Baroreflex Control. *Clinical and Experimental Pharmacology and Physiology,* 35**,** 987-994.
SILVANI, A., CALANDRA-BUONAURA, G., DAMPNEY, R. A. L. & CORTELLI, P. 2016. Brain–heart interactions: physiology and clinical implications. *Philosophical Transactions of the Royal Society A: Mathematical, Physical and Engineering Sciences,* 374**,** 20150181.
SILVANI, A. & DAMPNEY, R. A. L. 2013. Central control of cardiovascular function during sleep. *American Journal of Physiology-Heart and Circulatory Physiology,* 305**,** H1683-H1692.
SMITH, M. G. 2017. The impact of railway vibration and noise on sleep.
SMITH, M. G., ÖGREN, M., THORSSON, P., HUSSAIN-ALKHATEEB, L., PEDERSEN, E., FORSSÉN, J., AGEBORG MORSING, J. & PERSSON WAYE, K. 2020. A laboratory study on the effects of wind turbine noise on sleep: results of the polysomnographic WiTNES study. *Sleep*.
SOMMERMEYER, D., ZOU, D., EDER, D. N., HEDNER, J., FICKER, J. H., RANDERATH, W., PRIEGNITZ, C., PENZEL, T., FIETZE, I., SANNER, B. & GROTE, L. 2014. The use of overnight pulse wave analysis for recognition of cardiovascular risk factors and risk: a multicentric evaluation. *J Hypertens,* 32**,** 276-85.
SPIEGEL, K., LEPROULT, R. & VAN CAUTER, E. 1999. Impact of sleep debt on metabolic and endocrine function. *Lancet,* 354**,** 1435-9.

TASSI, P., SAREMI, M., SCHIMCHOWITSCH, S., ESCHENLAUER, A., ROHMER, O. & MUZET, A. 2010. Cardiovascular responses to railway noise during sleep in young and middle-aged adults. *Eur J Appl Physiol,* 108**,** 671-80.
TERRILL, P. I. 2020. A review of approaches for analysing obstructive sleep apnoea-related patterns in pulse oximetry data. *Respirology,* 25**,** 475-485.
THOMAS, R. J., MIETUS, J. E., PENG, C.-K. & GOLDBERGER, A. L. 2005. An electrocardiogram-based technique to assess cardiopulmonary coupling during sleep. *Sleep,* 28**,** 1151-1161.
THOMAS, R. J., WOOD, C. & BIANCHI, M. T. 2018. Cardiopulmonary coupling spectrogram as an ambulatory clinical biomarker of sleep stability and quality in health, sleep apnea, and insomnia. *Sleep,* 41**,** zsx196.
TIMIO, M., LIPPI, G., VENANZI, S., GENTILI, S., QUINTALIANI, G., VERDURA, C., MONARCA, C., SARONIO, P. & TIMIO, F. 1997. Blood Pressure Trend and Cardiovascular Events in Nuns in a Secluded Order: A 30-Year Follow-up Study. *Blood Pressure,* 6**,** 81-87.
VALLET, M., GAGNEUX, J. M., BLANCHET, V., FAVRE, B. & LABIALE, G. 1983. Long-Term Sleep Disturbance Due to Traffic Noise. *Journal of Sound and Vibration,* 90**,** 173-191.
VGONTZAS, A. N., ZOUMAKIS, E., BIXLER, E. O., LIN, H. M., FOLLETT, H., KALES, A. & CHROUSOS, G. P. 2004. Adverse effects of modest sleep restriction on sleepiness, performance, and inflammatory cytokines. *J Clin Endocrinol Metab,* 89**,** 2119-26.
WARBY, S. C., WENDT, S. L., WELINDER, P., MUNK, E. G., CARRILLO, O., SORENSEN, H. B., JENNUM, P., PEPPARD, P. E., PERONA, P. & MIGNOT, E. 2014. Sleep-spindle detection: crowdsourcing and evaluating performance of experts, non-experts and automated methods. *Nat Methods,* 11**,** 385-92.
WORLD HEALTH, O. 2018. Environmental Noise Guidelines for the European Region.
XU, L., ZHANG, D., WANG, K., LI, N. & WANG, X. 2007. Baseline wander correction in pulse waveforms using wavelet-based cascaded adaptive filter. *Comput Biol Med,* 37**,** 716-31.
YETTON, B. D., NIKNAZAR, M., DUGGAN, K. A., MCDEVITT, E. A., WHITEHURST, L. N., SATTARI, N. & MEDNICK, S. C. 2016. Automatic detection of rapid eye movements (REMs): A machine learning approach. *Journal of Neuroscience Methods,* 259**,** 72-82.
ZINCHUK, A. V., JEON, S., KOO, B. B., YAN, X., BRAVATA, D. M., QIN, L., SELIM, B. J., STROHL, K. P., REDEKER, N. S., CONCATO, J. & YAGGI, H. K. 2018. Polysomnographic phenotypes and their cardiovascular implications in obstructive sleep apnoea. *Thorax,* 73**,** 472-480.
ZOCCOLI, G. & AMICI, R. 2020. Sleep and autonomic nervous system. *Current Opinion in Physiology,* 15**,** 128-133.

APPENDIX A

Different amplitude ratio thresholds were applied to determine which one was the most appropriate. First of all, all standard deviations from the 2 different F1-score curves cross as shown in Figure A-1.

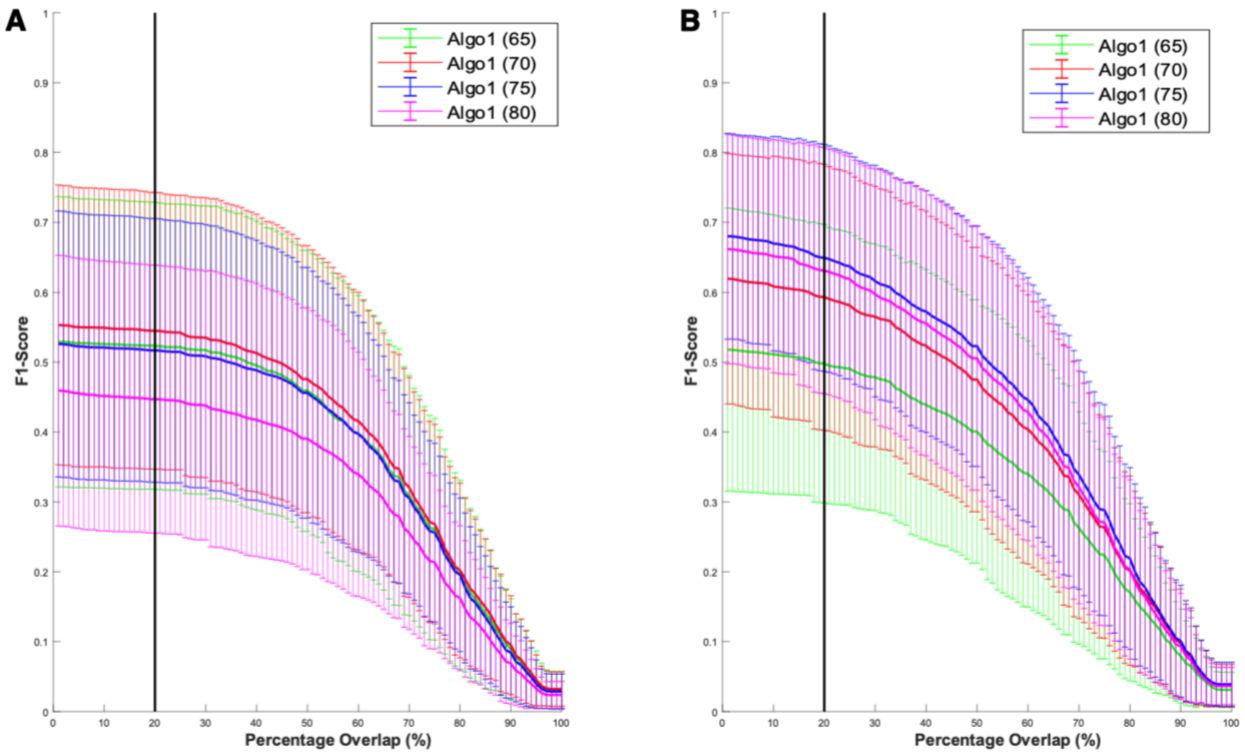

Figure A-1: The F1-score curves with standard deviation as a function of percentage overlap (%) during all sleep recordings. A) the "consensus" scoring agreement between scorers was the reference to construct the curves of both algorithms, and B) all scored PWA-drops of both scorers was the reference to construct the curves of both algorithms.

Another clearer figure was created with only the average F1-score curves to more easily observe the differences in amplitude ratio thresholds (Figure A-2). For the scoring agreement between scorers, the 70% amplitude ratio threshold had the higher mean F1-score curve (Figure A-2A) however, the 75% amplitude ratio threshold had a higher mean F1-score curve for the all scored PWA-drops from both scorers (Figure A-2B). Therefore, the 70% amplitude ratio threshold was more conservative than the 75% one. However, to be less conservative and to allow broader analysis in the future, the 75% amplitude ratio was retained as the amplitude ratio threshold.

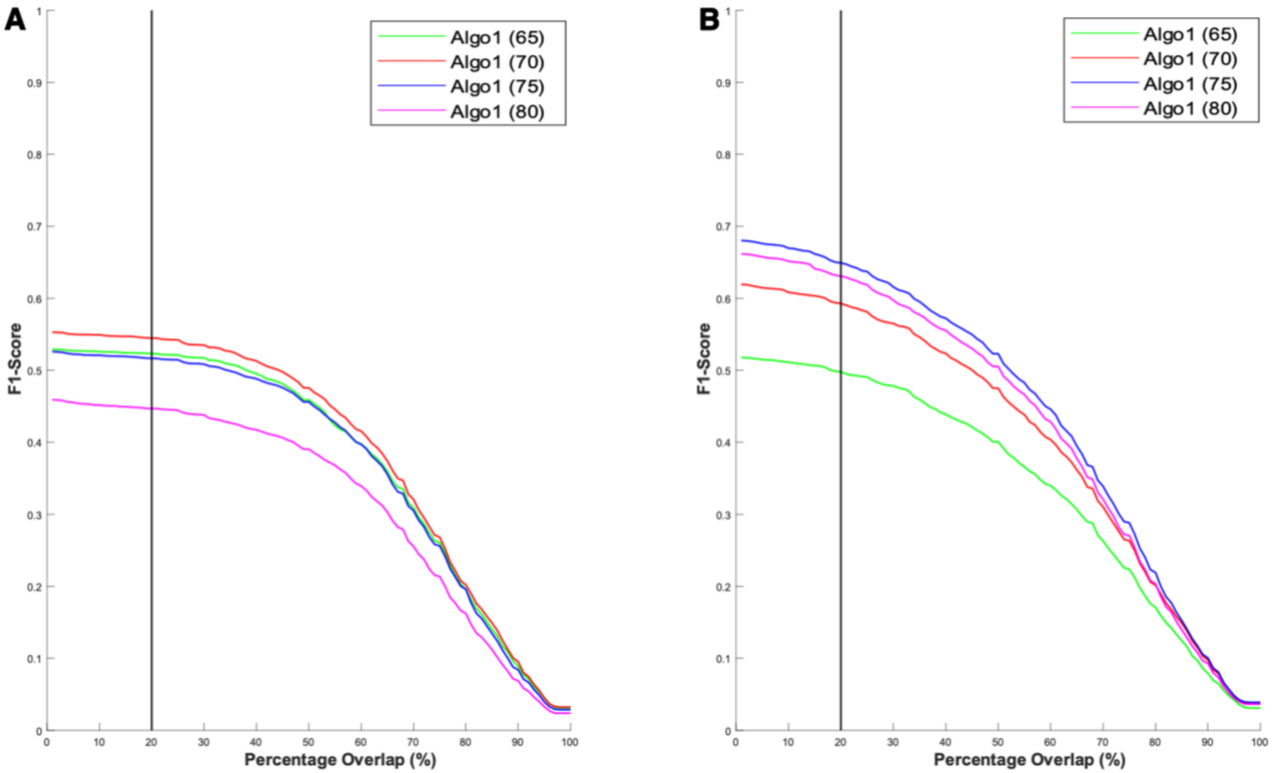

Figure A-2: The F1-score curves as a function of percentage overlap (%) during all sleep recordings. A) the “consensus” scoring agreement between scorers was the reference to construct the curves of both algorithms, and B) all scored PWA-drops of both scorers was the reference to construct the curves of both algorithms.

Table A-1: Performance of both algorithms for the percentage overlap of 20% expressed with mean and standard deviation.

Overlap Threshold (20%)		F1-Score	Precision	Recall
		Mean (± SD)		
The scoring agreement of both scorers	Envelope algorithm	0.49 (± 0.17)	0.37 (± 0.17)	0.81 (± 0.10)
	Moving window algorithm	0.51 (± 0.19)	0.42 (± 0.20)	0.71 (± 0.19)
All scored PWA-drop of both scorers	Envelope algorithm	0.64 (± 0.15)	0.62 (± 0.20)	0.70 (± 0.13)
	Moving window algorithm	0.64 (± 0.16)	0.71 (± 0.18)	0.62 (± 0.18)

APPENDIX B

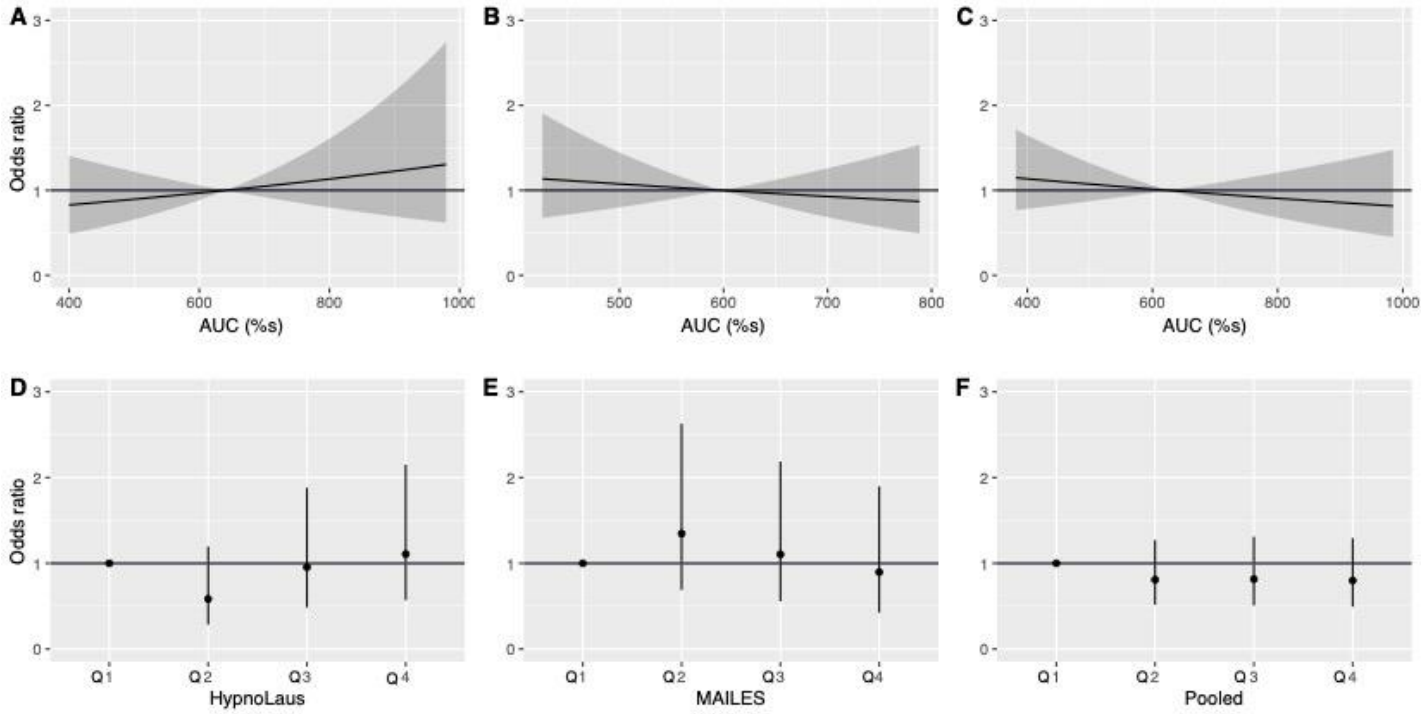

Figure B-1: PWA-drop mean AUC and CV events. Linear (A-C) and quartiles (D-F) odds ratios with 95% confidence intervals.

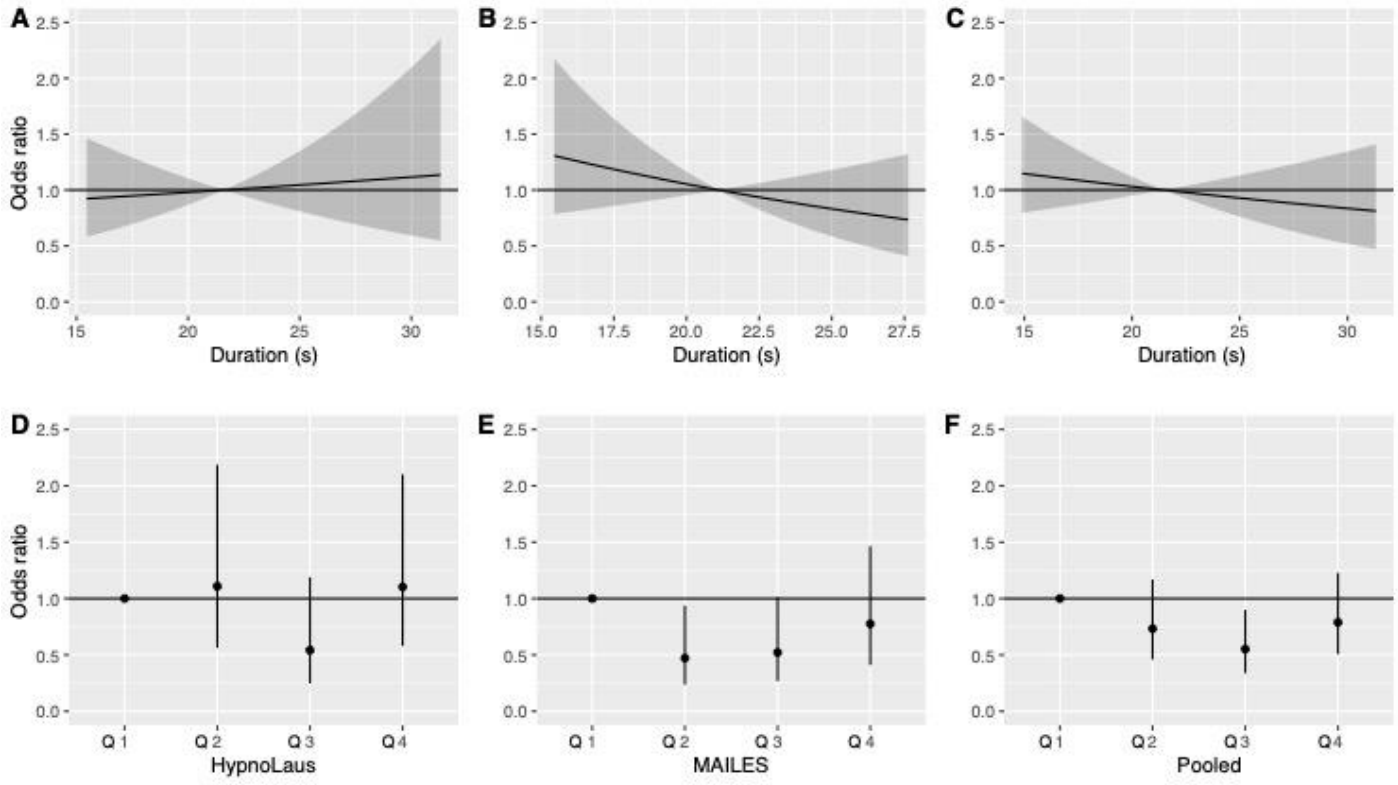

Figure B-2: PWA-drop mean duration and CV events. Linear (A-C) and quartiles (D-F) odds ratios with 95% confidence intervals.

Table B-1: Likelihood ratio test with and without PWA-drop features included in the models with CV event prevalence.

CV event prevalence	HypnoLaus	MAILES	Pooled
PWA-drop mean AUC	χ^2 = 0.48, p = 0.487	χ^2 = 0.26, p = 0.609	χ^2 = 0.07, p = 0.794
PWA-drop mean duration	χ^2 = 0.12, p = 0.734	χ^2 = 1.51, p = 0.220	χ^2 = 0.40, p = 0.527
PWA-drop mean index	χ^2 = 3.83, p = 0.050	χ^2 = 3.58, p = 0.059	χ^2 = 0.67, p = 0.412

Table B-2: Predictive performance of the models for hypertension prevalence associated with PWA-drop features using C-index (C) and Somers' Dxy indices corrected for optimism (O) using bootstrapping.

Hypertension prevalence	HypnoLaus	MAILES	Pooled
PWA-drop mean AUC	C = 0.80, Dxy = 0.60 and O = 0.01	C = 0.74, Dxy = 0.48 and O = 0.03	C = 0.79, Dxy = 0.59 and O < 0.01
PWA-drop mean duration	C = 0.80, Dxy = 0.60 and O < 0.01	C = 0.74, Dxy = 0.48 and O = 0.03	C = 0.79, Dxy = 0.58 and O < 0.01
PWA-drop mean index	C = 0.80, Dxy = 0.60 and O < 0.01	C = 0.74, Dxy = 0.48 and O = 0.03	C = 0.79, Dxy = 0.58 and O < 0.01

Table B-3: Predictive performance of the models for CV event prevalence associated with PWA-drop features using C-index (C) and Somers' Dxy indices corrected for optimism (O) using bootstrapping.

CV event prevalence	HypnoLaus	MAILES	Pooled
PWA-drop mean AUC	C = 0.82, Dxy = 0.65 and O = 0.04	C = 0.75, Dxy = 0.50 and O = 0.07	C = 0.81, Dxy = 0.62 and O = 0.03
PWA-drop mean duration	C = 0.82, Dxy = 0.65 and O = 0.04	C = 0.75, Dxy = 0.50 and O = 0.07	C =0.81, Dxy = 0.62 and O = 0.03
PWA-drop mean index	C = 0.82, Dxy = 0.65 and O = 0.03	C = 0.74, Dxy = 0.48 and O = 0.06	C = 0.81, Dxy = 0.62 and O = 0.03

Table B-4: Hypertension prevalence and PWA-drop features. Odds ratio by quartiles with 95% confidence intervals for the moving window algorithm developed in the second chapter.

Hypertension		**PWA-drop mean AUC**	**PWA-drop mean duration**	**PWA-drop mean index**
		OR [95% CI]	OR [95% CI]	OR [95% CI]
HypnoLaus	Q1	1.00	1.00	1.00
	Q2	0.97 [0.72-1.30]	0.95 [0.71-1.27]	0.66 [0.49-0.88]
	Q3	1.00 [0.74-1.35]	0.98 [0.72-1.33]	0.94 [0.70-1.25]
	Q4	1.42 [1.03-1.96]	1.15 [0.85-1.56]	0.65 [0.48-0.86]
MAILES	Q1	1.00	1.00	1.00
	Q2	0.96 [0.59-1.56]	1.15 [0.72-1.83]	1.20 [0.75-1.94]
	Q3	1.41 [0.85-2.33]	1.71 [1.07-2.74]	1.44 [0.90-2.33]
	Q4	1.84 [1.10-3.08]	1.41 [0.87-2.28]	1.30 [0.80-2.11]
Pooled	Q1	1.00	1.00	1.00
	Q2	0.99 [0.77-1.28]	1.10 [0.86-1.41]	0.91 [0.71-1.16]
	Q3	1.22 [0.94-1.57]	1.15 [0.89-1.48]	0.95 [0.75-1.22]
	Q4	1.58 [1.21-2.07]	1.29 [1.01-1.66]	0.95 [0.74-1.22]

Table B-5: CV event prevalence and PWA-drop features. Odds ratio by quartiles with 95% confidence intervals for the moving window algorithm developed in the second chapter.

CV event		PWA-drop mean AUC	PWA-drop mean duration	PWA-drop mean index
		OR [95% CI]	OR [95% CI]	OR [95% CI]
HypnoLaus	Q1	1.00	1.00	1.00
	Q2	0.58 [0.29-1.20]	1.11 [0.56-2.17]	0.51 [0.28-0.94]
	Q3	0.95 [0.48-1.88]	0.54 [0.25-1.19]	0.57 [0.30-1.08]
	Q4	1.11 [0.57-2.15]	1.10 [0.58-2.10]	0.40 [0.20-0.81]
MAILES	Q1	1.00	1.00	1.00
	Q2	1.32 [0.67-2.58]	0.44 [0.22-0.87]	1.83 [0.95-3.53]
	Q3	1.08 [0.54-2.15]	0.50 [0.25-0.97]	1.10 [0.54-2.25]
	Q4	0.87 [0.41-1.84]	0.71 [0.38-1.34]	1.56 [0.77-3.19]
Pooled	Q1	1.00	1.00	1.00
	Q2	0.83 [0.53-1.31]	0.72 [0.45-1.15]	0.94 [0.62-1.41]
	Q3	0.86 [0.53-1.38]	0.56 [0.34-0.91]	0.62 [0.38-1.01]
	Q4	0.90 [0.55-1.47]	0.82 [0.53-1.28]	0.73 [0.46-1.17]

Table B-6: Hypertension and CV event prevalence associated with PWA-drop features. Odds ratio with 95% confidence intervals for the moving window algorithm developed in the second chapter.

Moving window algorithm		Hypertension	CV event
		OR [95% CI]	OR [95% CI]
HypnoLaus	PWA-drop index (10 events/h decrease)	1.06 [0.99-1.13]	1.15 [0.99-1.32]
	PWA-drop mean duration (1 s increase)	1.03 [0.99-1.07]	1.01 [0.94-1.09]
	PWA-drop mean AUC (10%s increase)	1.01 [1.01-1.03]	1.01 [0.99-1.03]
MAILES	PWA-drop index (10 events/h decrease)	0.96 [0.86-1.08]	0.86 [0.73-1.01]
	PWA-drop mean duration (1 s increase)	1.07 [0.99-1.14]	0.95 [0.86-1.03]
	PWA-drop mean AUC (10%s increase)	1.03 [1.01-1.05]	0.99 [0.96-1.02]
Pooled	PWA-drop index (10 events/h decrease)	1.03 [0.97-1.09]	1.04 [0.94-1.16]
	PWA-drop mean duration (1 s increase)	1.04 [1.01-1.08]	0.98 [0.93-1.04]
	PWA-drop mean AUC (10%s increase)	1.02 [1.01-1.03]	0.99 [0.98-1.01]